

Rothamsted Repository Download

A - Papers appearing in refereed journals

Henry, C., Watson-Lazowski, A., Oszvald, M., Griffiths, C. A., Paul, M. J., Furbank, R. T. and Ghannoum, O. 2019. Sugar sensing responses to low and high light in leaves of the C4 model grass *Setaria viridis*. *Journal of Experimental Botany*.

The publisher's version can be accessed at:

- <https://dx.doi.org/10.1093/jxb/erz495>

The output can be accessed at: <https://repository.rothamsted.ac.uk/item/96xz3/sugar-sensing-responses-to-low-and-high-light-in-leaves-of-the-c4-model-grass-setaria-viridis>.

© 2 November 2019, Please contact library@rothamsted.ac.uk for copyright queries.

Sugar sensing responses to low and high light in leaves of the C₄ model grass *Setaria viridis*

Clémence Henry¹, Alexander Watson-Lazowski¹, Maria Oszvald², Cara Griffiths², Matthew J. Paul², Robert T. Furbank³ and Oula Ghannoum¹

¹ARC Centre of Excellence for Translational Photosynthesis, Hawkesbury Institute for the Environment, Western Sydney University, Locked Bag 1797, Penrith NSW 2751, Australia

²Plant Science, Rothamsted Research, West Common, Harpenden, Hertfordshire, AL5 2JQ, UK

³ARC Centre of Excellence for Translational Photosynthesis, Research School of Biology, Australian National University, Acton ACT 2601, Australia

Corresponding author contact details: Clémence Henry
clemence.henry84@gmail.com
+61 412 896 298

Other authors email:
a.watson-lazowski@westernsydney.edu.au
maria.oszvald@rothamsted.ac.uk
cara.griffiths@rothamsted.ac.uk
matthew.paul@rothamsted.ac.uk
robert.furbank@anu.edu.au
o.ghannoum@westernsydney.edu.au

© The Author(s) 2019. Published by Oxford University Press on behalf of the Society for Experimental Biology.

This is an Open Access article distributed under the terms of the Creative Commons Attribution Non-Commercial License (<http://creativecommons.org/licenses/by-nc/4.0/>), which permits non-commercial re-use, distribution, and reproduction in any medium, provided the original work is properly cited. For commercial re-use, please contact journals.permissions@oup.com

HIGHLIGHTS:

Low and high light contrastingly impact photosynthesis and sugar levels in C₄ source leaves of *Setaria viridis*, and elicit a different sugar sensing response relative to previous studies in C₃.

ABSTRACT:

Although sugar regulate photosynthesis, the signalling pathways underlying this process remain elusive, especially for C₄ crops. To address this knowledge gap and identify potential candidate genes, we treated *Setaria viridis* (C₄ model) plants acclimated to medium light intensity (ML, 500 $\mu\text{mol m}^{-2} \text{s}^{-1}$) with low (LL, 50 $\mu\text{mol m}^{-2} \text{s}^{-1}$) or high (HL, 1000 $\mu\text{mol m}^{-2} \text{s}^{-1}$) light for 4 days and observed the consequences on carbon metabolism and the transcriptome of source leaves. LL impaired photosynthesis and reduced leaf content of signalling sugars (glucose, sucrose and trehalose-6-phosphate). Contrastingly, HL strongly induced sugar accumulation without repressing photosynthesis. LL more profoundly impacted leaf transcriptome, including photosynthetic genes. LL and HL contrastingly altered the expression of HXK and SnRK1 sugar sensors and trehalose pathway genes. The expression of key target genes of HXK and SnRK1 were affected by LL and sugar depletion, while surprisingly HL and strong sugar accumulation only slightly repressed the SnRK1 signalling pathway. In conclusion, we demonstrate that LL profoundly impacted photosynthesis and the transcriptome of *S. viridis* source leaves, while HL altered sugar levels more than LL. We also present the first evidence that sugar signalling pathways in C₄ source leaves may respond to light intensity and sugar accumulation differently to C₃ source leaves.

KEY WORDS: C₄ photosynthesis; Glucose; Hexokinase (HXK); *Setaria viridis*; Sucrose; Sugar signalling; Sucrose-non fermenting 1 (Snf1) related protein kinase 1 (SnRK1); Target of rapamycin (TOR); Trehalose-6-phosphate

ABBREVIATIONS:

A_{net} : net photosynthetic rate

CCM: CO₂ concentrating mechanism

C_i : internal CO₂ concentration

DE: Differentially expressed

FC: Fold change

F_o : Minimal fluorescence signal (zero subtracted), dark adapted

F_o' : Minimal fluorescence signal (zero subtracted), light adapted

F_m' : Maximum fluorescence signal (zero subtracted), light adapted

F_s : Steady state fluorescence

g_s : stomatal conductance

HL: High light

HXK: Hexokinase

LL: Low light

ML: Medium light

NADP-ME: NADP-malic enzyme

PEPC: Phosphoenolpyruvate carboxylase

S6P: Sucrose-6P

SnRK1: Sucrose-non fermenting 1 (Snf1) related protein kinase 1

T6P: Trehalose-6-phosphate

TOR: Target of rapamycin

TPP: Trehalose-6-phosphate phosphatase

TPS: Trehalose-6-phosphate synthase

TRE: Trehalase

INTRODUCTION

Plant growth depends on sugar production in source leaves and sugar utilisation by sink tissues (e.g., grains, roots, young leaves). Photosynthesis and sink demand are tightly coordinated through metabolic and signalling feedback regulations. Sugar signalling integrates sugar production with plant development and environmental cues (Rolland *et al.*, 2006). In C₃ plants, sugar accumulation in source leaves, due to source-sink imbalance, negatively feedbacks on photosynthesis and plant productivity (Goldschmidt and Huber, 1992; Krapp and Stitt, 1995; Paul and Foyer, 2001; Paul and Pellny, 2003). However, we have a lack of understanding regarding the molecular mechanisms underlying those feedback regulations, especially in C₄ plants. Addressing this research gap is critical because improving crop yield requires a better understanding of how plants coordinate source activity with sink demand.

C₄ photosynthesis evolved from the ancestral C₃ pathway ~30 Mya following a drop in atmospheric CO₂ which limited the productivity of C₃ plants in warm climates (Sage *et al.*, 2012). During C₄ photosynthesis, CO₂ is concentrated around Rubisco, the rate-limiting enzyme of the Calvin (C₃) cycle through a CO₂ concentrating mechanism (CCM) to enhance the productivity and efficiency of C₄ plants (Hatch, 1987; Ghannoum *et al.*, 2011). About 50% of C₄ plants are grasses which include some of the world's major staple food, fodder and biofuel crops, such as maize, sugarcane, sorghum, millets, *Miscanthus* and switchgrass.

Hexokinase (HXK) was the first sugar sensor identified in plants (Jang and Sheen, 1994; Jang *et al.*, 1997) and is well known for its feedback regulation of photosynthesis and yield through its glucose signalling function. In maize mesophyll protoplasts, the activity of the promoter of seven photosynthetic genes was strongly repressed (3-20 fold) by high concentrations (300 mM) of glucose or sucrose (Sheen, 1990). Using sugar analogues, mutants and transgenic approaches, *AtHXK1* was shown to trigger the glucose repression of photosynthetic rates, stomatal conductance, photosynthetic genes expression, plant growth and yield (Jang *et al.*, 1997; Dai *et al.*, 1999; Xiao *et al.*, 2000; Moore *et al.*, 2003; Kelly *et al.*, 2012, 2013, 2014; Brauner *et al.*, 2015). Rice *OsHXK5* and *OsHXK6* were found to have a similar function to *AtHXK1*, showing that this pathway is conserved among plant species (Cho *et al.*, 2008). The role of HXK is yet to be confirmed in intact leaves of C₄ plants under physiological conditions.

The Target of Rapamycin (TOR) complex is another glucose sensor. TOR promotes plant development and growth under favourable environmental conditions (Dobrenel *et al.*, 2011; Henriques *et al.*, 2014; Rexin *et al.*, 2015; Xiong and Sheen, 2015). Studies using TOR-specific inhibitors, mutants and transgenic plants showed that the TOR complex is involved in the glucose-dependent induction of photosynthesis, water use efficiency, chlorophyll metabolism, photosynthetic gene expression, stress tolerance, growth and yield

(Xiong *et al.*, 2013; Dong *et al.*, 2015; Li *et al.*, 2015b; Xiong *et al.*, 2017; Bakshi *et al.*, 2017). However, a clear link between TOR and photosynthesis or growth of C₄ plants, is yet to be established.

The Sucrose-non fermenting 1 (Snf1) related protein kinase 1 (SnRK1) complex, is a starvation sensor, generally involved in stress response and survival, and usually acts antagonistically to the TOR complex (Tomé *et al.*, 2014; Li and Sheen, 2016; Baena-González and Hanson, 2017). The SnRK1 complex is directly inhibited by trehalose-6-phosphate (T6P), a sensing sugar which is a proxy for sucrose levels. SnRK1 becomes active under unfavourable environmental conditions to suppress growth and promote survival (Zhang *et al.*, 2009; Tomé *et al.*, 2014; Figueroa and Lunn, 2016; Griffiths *et al.*, 2016). Photosynthesis gene expression is activated by SnRK1 overexpression (Baena-Gonzalez *et al.*, 2007); however, there is limited evidence for a direct link between the SnRK1 complex activity and photosynthesis (Cho *et al.*, 2012; Nukarinen *et al.*, 2016).

Transgenic modification of T6P pathway in tobacco showed that increased leaf T6P content enhanced photosynthetic capacity per unit leaf area, whilst reducing leaf area and photosynthesis per plant (Pellny *et al.*, 2004). In maize with genetically impaired T6P accumulation in sink tissues, photosynthetic rates were indirectly increased in source leaves suggesting that T6P could mediate sink regulation of photosynthesis, perhaps through interaction with SnRK1 (Oszvald *et al.*, 2018). In maize source leaves, salt stress reduced photosynthesis whilst increasing sugar concentration (sucrose, glucose, and T6P only at silking stage), which resulted in the repression of SnRK1 *in vitro* activity but not in clear changes of key downstream targets of SnRK1 (Henry *et al.*, 2015).

The great majority of studies of the role of sugar signalling in photosynthesis have been conducted on C₃ plants such as Arabidopsis, tomato, tobacco, bean, wheat and rice. Only a few studies used C₄ species. In addition, a very limited number of studies have assessed how sugar signalling regulates photosynthesis through physiological or environmental alterations of sugar contents in intact plants (Bläsing *et al.*, 2005), as opposed to artificially feeding sugars. Sugar signalling in C₄ photosynthesis is important not only in the context of C₄ crop improvement, but also for bioengineering more productive C₃ crops with superior photosynthetic C₄ traits. Alongside transferring superior C₄ photosynthetic traits into major C₃ staple crops such as rice (Karki *et al.*, 2013; Wang *et al.*, 2016), we need a better understanding of how source activity and sink demand are coordinated in the complex C₄ mechanism. This includes fundamental differences in sugar signalling mechanisms that may exist between C₃ and C₄ plants, and the way they may impact photosynthesis, plant productivity and crop yield. The anatomical and biochemical specialisations needed to achieve a C₄ photosynthesis add complexities in extending a putative signalling model from C₃ to C₄ plants (Hatch, 1987; Lunn and Furbank, 1997, 1999; Leegood, 2000).

The overall aim of our study was to explore the relationship between photosynthesis and sugar signalling in C₄ plants. As sugar signalling mutants are not available in C₄ plants we used the C₄ model species *Setaria viridis* (green foxtail millet) to start identifying gene targets. *S. viridis* has recently become a genetic model species to study C₄ photosynthesis due to its small size, short life cycle, small sequenced genome, transformability and very close phylogenetic relationship with all the main C₄ crops belonging to the same NADP-ME subtype (Brutnell *et al.*, 2010; Li and Brutnell, 2011; Pant *et al.*, 2016). Here, we induced endogenous strong and rapid physiological changes in sugar levels and photosynthesis in C₄ source leaves by varying light intensity over four days using low (50 $\mu\text{mol m}^{-2} \text{s}^{-1}$) and high (1000 $\mu\text{mol m}^{-2} \text{s}^{-1}$) light intensities. We focussed on the source leaf to directly explore the relationship between sugar signalling and photosynthesis.

MATERIAL AND METHODS

Plant material, growth conditions and sampling

Wild type *Setaria viridis* A10 seeds (stock from Hugo Alonso Cantabrana, ANU, Canberra, Australia) were treated for 24h at 28°C with 5% liquid smoke (Hickory, Wright's, USA) to release dormancy (Sebastian *et al.*, 2014). Several seeds were planted ~2 cm below ground in 0.3L (9 cm top/7.5 cm base x 10 cm height) black plastic pots (Reko, Australia) filled with "Osmocote seed raising and cutting mix" (Scotts, Australia), sprayed with water from top (regularly for the first few days only to ensure good germination) and placed in trays filled halfway with nutrient solution (0.8g L⁻¹ of Thrive all-purpose soluble fertiliser, Yates, Australia). Plants were grown for 3 weeks in 3 separate reach-in growth cabinets (GC-20-BDAF model, BioChambers, Canada) under the following conditions: 500 $\mu\text{mol m}^{-2} \text{s}^{-1}$ (measured at canopy level) of light provided by a mix of 6 400w high pressure sodium (HPS) lamps and 6 400w Metal Halide (MH) lamps; 16h day: 8h night, 28°C day: 22°C night; 400 ppm CO₂ and 60% relative humidity (control conditions). To ensure full homogeneity between the chambers, plants were rotated weekly between and within the chambers for the first 3 weeks. Two weeks after planting, fungicide treatment (5g L⁻¹ Mancozeb plus, Yates) was gently sprayed on the canopy to prevent pathogenic infection. Three weeks after planting, treatments started by changing the light intensity in the chambers to LL (50 $\mu\text{mol m}^{-2} \text{s}^{-1}$), ML (500 $\mu\text{mol m}^{-2} \text{s}^{-1}$) or HL (1000 $\mu\text{mol m}^{-2} \text{s}^{-1}$) respectively, with the same photoperiod, temperature and relative humidity as before, for 4 consecutive days. Measurements and sampling were made from day 0 (before treatment) to day 4.

Photosynthetic measurements

Leaf photosynthesis, internal CO₂ concentration and stomatal conductance were determined using the LI-6400XT open gas-exchange system coupled to the 6400-40 leaf

chamber fluorometer (Licor, Lincoln, USA). For each treatment and time point, measurements were taken on the mid-section of the last fully expanded leaf on the main shoot of 4-5 independent plants. Measurements were carried between 9 AM and 4 PM (1-8h after lights were turned on). Gas exchange instruments were randomised between plants, treatments and days. Leaf area was measured using engineering paper before clamping the leaf in the chamber.

Maximal leaf photosynthetic capacity and fluorescence (F_o , F_s , F_m' and F_o') were measured at high light intensity of $1000 \mu\text{mol m}^{-2} \text{s}^{-1}$ (with 10% blue), reference CO_2 concentration of 400 ppm, leaf temperature of 28°C and relative humidity of ~50-60%. Measurements were auto-logged every minute for 45-150 min depending on the treatment, with IRGAs matched every 2 min. Once leaves reached a steady state, maximum photosynthesis and fluorescence were measured. Plants exposed to LL took progressively longer to reach steady state. Subsequently, A_{net}/C_i response curves were measured by gradually changing CO_2 concentration in the leaf chamber as follows: 50, 100, 150, 200, 300, 400, 600, 800, 1200, 1800 and 400 ppm.

Photosynthesis and fluorescence were also measured at growth light intensity of 500 (day 0) and 50 (LL), 500 (ML) or 1000 (HL) $\mu\text{mol m}^{-2} \text{s}^{-1}$ (day 1-4) depending on the treatments. Other conditions were kept the same as described above.

Photosynthetic enzymes *in vitro* assays, western blots and chlorophyll content determination

Samples were collected in the light and leaf area measured before they were snap frozen in liquid N_2 and stored at -80°C . To measure PEPC, NADP-ME and Rubisco activity we used a method adapted from (Sharwood *et al.*, 2016b). Briefly, leaf soluble proteins were extracted in a N_2 -sparged extraction buffer (50 mM EPPS-NaOH pH 7.8, 5 mM MgCl_2 , 1 mM EDTA, 5 mM DTT, 1% (w/v) PVPP and 1% (v/v) plant protease inhibitor cocktail [Sigma-Aldrich]) from frozen samples. Soluble proteins (10 μL) were then added to a reaction mix to 485 μL of PEPC (50 mM EPPS-NaOH pH 8, 0.5 mM EDTA, 0.2 mM NADH, 5 mM Glucose-6-P, 1 mM NaHCO_3 , 0.5 U MDH and 10 mM MgCl_2), NADP-ME (49.25 mM Tricine-KOH pH 8.3, 4 mM MgCl_2 , 0.5 mM NADP and 0.1 mM EDTA) or Rubisco (50 mM EPPS-NaOH pH 8, 0.5 mM EDTA, 0.2 mM NADH, 1 mM ATP, 5 mM Creatine phosphate, 20 mM NaHCO_3 , 10 μL coupling enzymes and 10 mM MgCl_2) reaction buffers incubated at 25°C . PEPC, NADP-ME and Rubisco reactions were then started by adding 5 μL of PEP (4 mM final), malate (5 mM final) or RuBP (0.22 mM final), respectively. The NAD^+/H reduction or oxidation were then monitored at 340 nm and the initial slopes were used to calculate the enzyme activities (Sharwood *et al.*, 2014, 2016a) (**Protocol S1**). In addition, 300 μL of the fresh soluble fraction extracted for the assay was mixed with 100 μL of NuPAGE LDS Sample Buffer (4x)

(Life Technologies), snap frozen in liquid N₂ and stored at -80°C for SDS-PAGE and western blot analysis. SDS-PAGE and Immunoblot analysis of photosynthetic proteins (PEPC, NADP-ME and Rubisco) were carried out as in (Sharwood *et al.*, 2014) (**Protocol S2**).

Protein content in soluble extract was determined by using the Pierce™ Coomassie Plus (Bradford) Assay Reagent (Thermo Scientific), BSA as a standard, 96 well plates and the CLARIOstar Microplate Reader (BMG LabTech Pty Ltd). Chlorophyll content was determined using 100 µL of crude extract from the tissue lysate used for the enzymatic assays and western blots according to the acetone extraction and quantification method described by (Porra *et al.*, 1989).

Analysis of metabolites and *in vitro* SnRK1 activity

Measurements of glucose, fructose, sucrose, sucrose-6P (S6P), trehalose-6P (T6P) and trehalose were performed by Metabolomic Discoveries (Germany) using the method described by (Kretzschmar *et al.*, 2015). Briefly, metabolites were extracted from frozen leaf tissues and analysed by LC-MS. Measurements were then compared to samples from ML-day 0 plants (control) and adjusted for fresh weight. Measurements were performed on 4 independent biological replicates for each treatment and time point.

SnRK1 *in vitro* activity was determined using a method adapted from (Zhang *et al.*, 2009). 150-300mg of frozen leaf samples were ground in liquid N₂ and homogenized in ice-cold extraction buffer (100 mM Tricine-NaOH pH 8.2, 25 mM Sodium fluoride, 0.5 mM EGTA, 0.5 mM EDTA, 1 mM Benzamidine, 5 mM DTT, 20% (w/v) PVPP, 1X Protease inhibitor cocktail [PIC, P9599, Sigma-Aldrich] and 0.5X General non-specific phosphatase inhibitor cocktail [500 mM Sodium fluoride, 250 mM β-glycerophosphate, 100 mM Sodium pyrophosphate, 20 mM Sodium orthovanadate]). After centrifugation, soluble protein extracts were desalted through a NAP-10 column (GE Healthcare, UK) pre-equilibrated with resuspension buffer (100 mM Tricine-NaOH pH 8.2, 25 mM Sodium fluoride, 0.5 mM EGTA, 0.5 mM EDTA, 1 mM Benzamidine, 5 mM DTT) and resuspended in 1.5 mL of resuspension buffer added with 1X Protease inhibitor cocktail and 1 µM Okadaic acid. Soluble protein extracts were then aliquoted, freeze-snapped in liquid N₂ and stored at -80 °C until used for the assays. SnRK1 activities were determined in a final volume of 25 µL in microtiter plate wells at 30 °C. Assay medium contained 40 mM HEPES-NaOH pH 7.5, 5 mM MgCl₂, 4 mM DTT, 0.5 µM Okadaic acid, 1X PIC, 200 µM ATP containing 12.5 kBq of [γ-³³P]ATP (PerkinElmer), added with or without (negative control) 200 mM of AMARA peptide (Enzo Life Science). For trehalose-6-phosphate (T6P) inhibition assays, a final concentration of 1 mM T6P (T4272, Sigma-Aldrich) was added to the mix. Assays were started with the addition of 5 µL of protein extract and stopped after 4 min by transferring 15 µL of reaction mix to 2 cm² Protran 0.45 µm

nitrocellulose membrane (GE) immediately immersed in ultra-purified water. Membranes were then washed 4 times with 800 mL of ultra-purified water, air dried and transferred to 5 mL scintillation vials with 3.5 mL of scintillation cocktail (Ultima Gold). Radioactivity was then determined using a scintillation counter. For each time point, the assays were performed on 4 independent biological replicates in duplicates or triplicates.

Next generation RNA sequencing and functional gene annotation

Total RNA were extracted from ~10 mg finely ground frozen source leaf samples (collected at the same time as samples used for enzyme assays above) using Purezol (Biorad), resuspended in 50 μ L of RNA secure resuspension solution (Ambion) and stored at -80°C. Aliquots of RNA from each sample were then treated with DNase I (AMBION) following the manufacturer's protocols, before library preparation using a TruSeq Stranded RNA HT Kit for Plants (Illumina) was carried. RNA sequencing was then carried out using a Illumina Hi-Seq 2500 machine with 125 base pair paired-end sequencing by the Western Sydney University Next Generation Sequencing facility. Between 17 and 25 million reads were returned per sample. Raw reads can be found on GenBank under BioProject accession number PRJNA493674. Raw reads were pre-processed using Trimmomatic (Bolger *et al.*, 2014) to trim adapters. Transcript expression was calculated via mapping the processed reads to the closely related *S. italica* transcriptome (v2.2) (Bennetzen *et al.*, 2012) using DEW (<http://dew.sourceforge.net/>), an automated pipeline which utilises Bowtie2 (Langmead and Salzberg, 2012) to align reads against a given reference, then eXpress (Roberts and Pachter, 2013) to calculate normalised transcript expression (transcripts per million; TPM). Differentially expressed (DE) transcripts were identified using DEApp (Li and Andrade, 2017) utilising DESeq2 (Love *et al.*, 2014). A minimum read count of 1 count per million in at least two replicates and a false discovery rate (FDR) cut-off of ≤ 0.05 were used to identify DE transcripts. In order to not be overly stringent we chose not apply a minimum threshold in terms of fold change (FC), but instead to classify all DE transcripts into three groups: slightly (below 2 FC), mildly (between 2 and 5 FC) and highly (above 5 FC) DE transcripts. Heat maps were then generated using these groups. The exact FC of each DE transcript and the group to which they belong can be found in Table S5.

Predicted protein sequences are readily available for the *S. italica* genome v2.2 (Foxtail millet, <https://phytozome.jgi.doe.gov/pz/portal.html>) (Bennetzen *et al.*, 2012) and so were used to annotate all transcripts identified in our experiments. In addition of the pre-existing annotations of *S. italica* proteins, we used Mercator4 (beta version, <http://www.plabipd.de/portal/web/quest/mercator-ii-alpha-version->) (Lohse *et al.*, 2014) in order to obtain the Mapman 4 (Thimm *et al.*, 2004) annotation for each protein. Additional S.

italica transcripts were also annotated as C₄ photosynthetic genes, sugar sensors, trehalose pathway genes and putative sugar signalling targets (**Tables S6-12**) were determined using published RNA-Seq and microarray data from both Arabidopsis and C₄ grasses (Jang and Sheen, 1994; Jang *et al.*, 1997; Zhou *et al.*, 1998; Sheen *et al.*, 1999; Xiao *et al.*, 2000; Sung *et al.*, 2001; Krishna and Gloor, 2001; Moore *et al.*, 2003; Baena-Gonzalez *et al.*, 2007; Nishimura *et al.*, 2008; Andrès *et al.*, 2010; Flores-Pérez and Jarvis, 2013; Kikuchi *et al.*, 2013; Caldana *et al.*, 2013; Xiong *et al.*, 2013; Nunes *et al.*, 2013; John *et al.*, 2014; Kunz *et al.*, 2014, 2015; Trösch *et al.*, 2015; Nakai, 2015; Sharwood *et al.*, 2016a; Bracher *et al.*, 2017; Watson-Lazowski *et al.*, 2018) (studies used detailed in **Protocol S3**). For the sugar sensing targets, only those that behaved consistently within multiple studies were selected and annotated as such.

Statistical analysis

To assess significant changes in morphological, physiological and biochemical results, we performed a two-way ANOVA followed by a F-test using R (R Core Team, 2016) and RStudio (RStudio Team, 2015) to assess the effect of both treatment and time, as well as their interaction on each of the tested parameters. We also ensured that the distribution of the ANOVA was “normal” using a Quantile-Quantile Plot (qqPlot). To assess the effect of low and high light treatments compared to medium light control for each time point, we performed a one-way ANOVA followed by a Tukey test. For each parameter tested, we indicated significant differences ($p < 0.05$) between the treatments and the control with a star.

RESULTS

To quickly and strongly alter *in vivo* sugar levels and trigger related changes in sugar signalling and photosynthesis in C₄ leaves, we treated 3 week-old *S. viridis* plants acclimated to ML intensity ($500 \mu\text{mol m}^{-2} \text{s}^{-1}$, control) with low or high light intensity (LL = 50 or HL = $1000 \mu\text{mol m}^{-2} \text{s}^{-1}$, respectively) (**Fig. S1A**). Based on our preliminary experiments, four days of treatment were required and sufficient to trigger significant changes in sugar levels and photosynthetic capacity (**Fig. 1-2**), validating the experimental system used here.

LL strongly impaired photosynthesis of *S. viridis*, while HL had little effect

By day 4, LL treated plants had reduced growth and turgor, while HL treated plants showed the opposite effect when compared to control (ML) plants (**Fig. S1B**). In control and HL treated *S. viridis*, leaves typically took 25 min to reach steady-state photosynthesis (A_{net}) measured at high irradiance ($1000 \mu\text{mol m}^{-2} \text{s}^{-1}$) (**Fig. S2**). From day 1, LL strongly delayed (up to 150 min) the time for leaves to reach steady-state A_{net} at high irradiance (**Fig. S2**).

After 25 min of equilibration, LL reduced A_{net} (-65%) and stomatal conductance, g_s (-55%), and increased internal CO_2 concentration, C_i (+75%) starting from day 2 when compared to the control (**Fig. 1A-C**). When leaves were allowed to fully adjust to high irradiance, LL significantly reduced steady-state A_{net} (-27%) and g_s (-19%), and increased C_i (+36%) on day 4 only (**Fig. 1D-F**), indicating the onset of photosynthetic impairment. Reduced photosynthetic capacity on day 4 under LL, following full acclimation to high irradiance (**Fig. 1D-F**), was correlated with significant reductions in the initial slope (-49%) and maximum rate (-26%) of the A - C_i curves relative to the control (**Table S1, Fig. S3**), as well as fluorescence parameters (F_v/F_m' and ETR) (**Table S1**). In contrast, HL had no effect on any of the photosynthetic parameters (**Fig. 1, S3, Table S1**).

When measured at growth irradiance, photosynthesis and electron transport rates were near zero in LL plants, which also had higher maximum efficiency of PSII (F_v/F_m') and photochemical quenching (q_P) relative to the control. HL plants had slightly higher photosynthesis and electron transport rates when measured at growth light, but lower F_v/F_m' and q_P relative to control plants (**Fig. 1G-I, Table S1**).

LL induced a gradual decrease (\sim -50%) in the activity and content of PEPC (day 2) and NADP-ME (day 3) and the activation state of Rubisco (day 1) relative to control plants. HL increased the *in vitro* activity and content of PEPC (significantly by day 3) but had no significant effect on NADP-ME or Rubisco relative to the control (**Fig. S4**). Chlorophyll content was unaffected by the light treatment, and hence cannot explain the observed photosynthetic changes (**Table S1**).

HL had a greater impact than LL on the content of signalling sugars

LL gradually reduced the relative content of key sugars involved in sugar signalling (glucose, sucrose and trehalose-6-phosphate, T6P) as well as other key sugars (fructose, sucrose-6-phosphate and trehalose), while HL caused a strong gradual increase in sugar accumulation relative to the control (**Fig. 2, S5**). The relationship between photosynthesis measured at growth light and sugar content was exponential; photosynthesis and sugars increased abruptly from LL to ML, then photosynthesis plateaued with further sugar increases between ML and HL (**data not shown**).

SnRK1 starvation sensor was indirectly modulated by changes in T6P content, but not directly by the light treatment

The *in vitro* kinase (total or T6P-inhibited) activities of SnRK1 were generally unaffected by the light treatment over the course of the experiment. Addition of T6P (1 mM) to the reaction mix reduced the SnRK1 *in vitro* kinase activity to 30-65% of the total activity in all samples (**Fig. 3**). No correlation was found between photosynthetic rates at growth light

and the total or T6P-inhibited activity of SnRK1 (**data not shown**). However, *in vivo* changes in T6P content under LL and HL were associated with altered expression of key SnRK1 downstream targets, favouring activation and repression of SnRK1 under LL and HL, respectively (**Fig. 2, 6**). These results suggest that SnRK1 activity in *S. viridis* leaves was modulated through changes in T6P contents rather than through a direct modulation of the kinase activity by light in our experimental system.

LL induced major transcriptomic changes, especially for photosynthetic genes, while HL had little impact

On day 0, only 0-3 genes were differentially expressed (DE) between the treated plants and the controls, demonstrating that observed responses on subsequent days were caused by the light treatments and not due to random variations between replicates. At the whole transcriptome level, 7905 out of 17459 transcripts (45%) were significantly differentially expressed at LL and/or HL relative to control (**Fig. S6, Table S2**). LL significantly changed the expression of 4608, 3398 and 4373 transcripts on day 1, 2 and 4, respectively. In contrast, HL had limited to no effect on gene expression, with most of the changes occurring on day 1 (1426 DE transcripts) and very little changes observed on day 2 and 4 (191 and 69 DE transcripts, respectively) (**Table S2**).

LL (especially on days 2 and 4) down-regulated the expression of genes involved in photosynthesis, cellular respiration, metabolism of carbohydrate, amino acid, lipid, nucleotide, coenzyme, secondary and reactive oxygen, protein biosynthesis, cell wall, solute transport, and nutrient uptake (**Table S3**). LL up-regulated genes involved in chromatin assembly and remodelling, cell cycle, RNA biosynthesis, and membrane trafficking. Genes involved in protein degradation, phytohormones, cytoskeleton, protein translocation and DNA damage response were down- or up-regulated in equal numbers by LL. These changes are consistent with a general switch from anabolism to catabolism under low energy status and limited growth (**Fig. S1**).

On day 1, HL down-regulated the expression of genes involved in RNA biosynthesis, protein degradation, solute transport, phytohormones and nutrient uptake; and up-regulated the expression of genes involved in protein biosynthesis and translocation, RNA processing, cellular division, carbohydrate, amino acid and nucleotide metabolism, chromatin assembly and remodelling, cell cycle, and membrane vesicle trafficking (**Table S3**). Some genes involved in protein modification, environmental stimuli response, cell wall, cytoskeleton, coenzyme metabolism and reactive oxygen metabolism, and photosynthesis were down- or up-regulated in equal numbers by HL. These changes are generally consistent with increased anabolism leading to increased growth (**Fig. S1**).

Out of the 301 photosynthetic genes identified, LL respectively down- and up-regulated 74% and 4% of those genes; while HL respectively down- and up-regulated 2% and 4% of these genes (**Fig. 4, Table S2**). This demonstrates the profound inhibitory effect of LL on photosynthesis, which led to the observed sugar depletion, as opposed to the minor effects of HL on photosynthesis which was associated with large sugar accumulation in *S. viridis*.

LL and HL contrastingly altered the expression of key sugar signalling and trehalose pathway genes

Overall, light treatments significantly ($FDR \leq 0.05$) altered the expression of 42% of the 52 sugar signalling genes identified as expressed in *S. viridis* leaves. Once again, LL had a prominent effect on most of these genes, affecting 40% of them, while HL had a smaller and antagonist effect on them, with only 17% of those genes being affected (**Fig. 5, Table S2**).

In terms of the sugar sensors, LL repressed the expression of *SvHXK5* and 6, the closest homologs of the *HXK* isoforms able to sense glucose in Arabidopsis and rice. LL also induced the expression of several genes encoding key subunits of both the TOR and SnRK1 energy signalling complexes. On the other hand, HL had no effect on *HXK* or TOR complex genes, while it repressed the expression of two genes involved in the SnRK1 complex (**Fig. 5**).

In the trehalose pathway, LL strongly repressed the expression of both transcripts encoding the *TPSI.1* (TPS Class I) protein, which is responsible for the synthesis of T6P. In addition, LL induced the expression of several *TPSII* (TPS Class II), one *TPP* and *TRE* transcripts (**Fig. 5**), which are respectively potentially responsible for the regulation of *TPSI.1*, the dephosphorylation of T6P to form trehalose, and the degradation of trehalose into 2 glucose moieties (Ramon and Rolland, 2007). These changes are consistent with a reduction in T6P biosynthesis and an increase in T6P degradation, which explains the observed reduction in T6P levels under LL (**Fig. 2**). HL did not alter the expression of *TPSI.1* or *TRE*, but it repressed the expression of most *TPSII* which were induced under LL, as well as the expression of *TPPB.1.2* (**Fig. 5**). These results partly explain the strong increase of T6P levels observed under HL (**Fig. 2C**). In addition, *AtTPS8-10* *TPSII* genes are starvation inducible and sugar repressible (Nunes *et al.*, 2013), which is consistent with the respective induction and repression of six and five of the *TPSII* transcripts by LL and HL, respectively in our experiment (**Fig. 5**).

The expression of key sugar signalling target genes indicated the induction of both the SnRK1 and HXK-dependent signalling pathways by LL, while HL only slightly repressed the SnRK1 pathway

LL clearly altered the expression of well-characterised key downstream targets of both the SnRK1 and HXK-dependent sugar signalling pathways, indicating the activation of both these pathways under LL and sugar depletion in C₄ source leaves, while the TOR signalling pathway was clearly unaffected by LL (**Fig. 6, Table S2**). When considering the full list of putative SnRK1 downstream targets based on protein homology with genes identified in previously published work using C₃ plants, trends were less clear than for the well-characterised targets (**Fig. S6**). The discrepancy may relate to our focus on the source leaf, while most previous studies used *Arabidopsis* seedlings and sink tissues (e.g. wheat grain, Martínez-Barajas *et al.*, 2011) and/or protoplasts. Using the same list of key HXK, TOR and SnRK1 downstream targets, HL and sugar accumulation slightly repressed the SnRK1 signalling pathway only, but had no clear effect on either the HXK-dependent or the TOR signalling pathways (**Fig. 6**). Similar to LL, HL did not have a strong effect on the full list of SnRK1 downstream targets, although it induced a marginal (8-34 % of the total transcripts) change in the expression of the putative sugar signalling target genes (**Fig. S6, Table S2**). Taken together, our results suggest that, although LL may have induced the SnRK1 signalling pathway through changes in T6P levels in the C₄ source leaves, LL appears to have triggered a different overall sugar signalling response to that previously described in *Arabidopsis* (C₃). This indicates that the overall set of target genes affected by SnRK1 may differ between organisms (C₃ vs C₄), tissues (sink vs source) and/or development stages (vegetative vs mature stage).

DISCUSSION

Sugar feedback inhibition of C₃ photosynthesis and the role of sugar signalling in controlling sink development have been well studied, but the interplay between sugar signalling and C₄ photosynthesis remains poorly understood. Our study aimed at elucidating this knowledge gap by inducing concurrent changes in photosynthesis and sugar contents at varying light intensity. We hypothesised that C₄ photosynthesis might be less sensitive to sugar feedback inhibition than C₃ photosynthesis due to the fundamental differences between the way these species operate and regulate their sugar metabolism. Our study revealed two key novel findings. Firstly, LL impacted C₄ photosynthesis and the transcriptome of *S. viridis* source leaves more profoundly than HL, even though HL altered sugar levels to a greater extent than LL. Secondly, sugar signalling pathways of C₄ source leaves responded to light intensity and associated sugar accumulation differently to previous reports for C₃ plants using sink tissues, seedlings or protoplasts. Our results are highly relevant for the improvement of crop yield through a better understanding of the pathways regulating sugar production and allocation in source tissues.

LL impacted photosynthesis and transcriptome of *S. viridis* source leaves more profoundly than HL, while HL altered sugar levels more than LL

Four days after switching the light intensity, LL profoundly impacted three broad areas: (1) photosynthesis (photosynthetic rates, capacity, enzyme activity and content, and gene expression), (2) sugar metabolism and (3) gene expression of sugar signalling components (HXK, SnRK1 and the trehalose pathway), some of their targets and the whole transcriptome of C₄ source leaves. In contrast, the main effects of HL were a strong accumulation of sugars without any feedback regulation of photosynthesis and a slight repression of the SnRK1 pathway (**Fig. 1-6, S2, S4, Table S2**). C₄ species evolved and are adapted to high light (Sage and Percy, 2000). In addition, the operation of the CCM and overcycling of CO₂ into the bundle sheath requires additional energy (Hatch, 1987). This partly explains why C₄ plants are generally more sensitive to LL than HL (Usuda and Edwards, 1984; Usuda *et al.*, 1985, 1987; Kalt-Torres *et al.*, 1987).

LL reduced photosynthetic rates of C₄ source leaves to near zero, depleting sugars to very low levels (**Fig. 1-2**) and reducing plant growth and turgor (**Fig. S1**). Consequently, LL triggered massive and persistent transcriptional changes aimed at promoting cell maintenance and survival (**Fig. 7, Table S3**). In particular, photosynthetic enzymes and 74% of photosynthetic genes were repressed by LL (**Fig. 4, S4, Table S2**). Gene transcription and protein translation are energetically costly processes minimised under energy limitation (Baena-González, 2010; Browning and Bailey-Serres, 2015; Merchante *et al.*, 2017). At the

whole transcriptome level, LL also triggered a general down-regulation of genes involved in anabolism, and an up-regulation of genes involved in catabolism and gene/protein regulation, especially on day 4 (**Fig. 7, Table S3**). These results are consistent with previous work done on *C₃* plants, where transcriptome was strongly affected by prolonged shading (Gong *et al.*, 2014; Ding *et al.*, 2016).

In contrast to LL, HL had little effect on photosynthetic capacity, enzyme activity or gene expression of *S. viridis* source leaves. Although photosynthetic rates measured at growth light were slightly (+14-26%) increased by HL, HL induced a gradual and strong sugar accumulation (up to 4-8 fold on day 4) without inducing any photosynthetic downregulation (**Fig. 1-2**). At the whole transcriptome level, HL altered transcript abundance of 3 times fewer genes than LL on day 1, and of only very few genes on days 2 or 4 (**Fig. S6, Table S3**). On day 1, HL mainly induced transcriptional changes which promoted anabolism without impacting photosynthesis or sugar signalling. Subsequently, HL leaves regained physiological and transcriptional homeostasis while sugars continued to accumulate. Our results contrast with the usual photosynthetic repression associated with the exposure of *C₃* leaves to conditions leading to sugar accumulation (Sheen, 1990; Jang and Sheen, 1994; Jang *et al.*, 1997; Dai *et al.*, 1999; Xiao *et al.*, 2000; Kelly *et al.*, 2012).

LL and HL altered sugar levels and elicited unexpected sugar signalling responses in *C₄* source leaves that could be due to different sensitivities to sugars, alternate sugar or light signalling pathways

LL altered the expression of key sugar sensors more than HL (**Fig. 5**). However, despite the strong changes in glucose and T6P levels under both light treatments (**Fig. 2**), we did not observe all the expected sugar signalling responses (**Fig. 6, Table S2**). LL altered the transcript abundance of genes encoding HXKs and various components of TOR, SnRK1 and the trehalose pathway. LL also altered the expression of key downstream targets of HXK and SnRK1, indicating that both signalling pathways may be activated under low energy status (**Fig. 7**). Since most of the downstream targets of HXK are photosynthetic genes, which may also be regulated by light, it was difficult to separate the effects of the sugar- and light-dependent pathways. This point is addressed later in the manuscript.

On the other hand, according to the expression of well defined sugar sensing target genes, the strong glucose accumulation observed under HL did not associate with the activation of the HXK-dependent or the TOR signalling pathway expected under feast-like conditions (**Fig. 2, 5-7**). It was especially surprising for the HXK-dependent signalling pathway which typically associates with the feedback inhibition of photosynthesis (Sheen, 1990). Interestingly, the SnRK1 pathway seemed to be slightly repressed under HL, which agrees with the observed increase in T6P levels under HL (**Fig. 2, 9**) and its known inhibitory

effect on SnRK1 activity. SnRK1 extracted from source leaves is typically much less inhibited by T6P than in sink tissues (Zhang *et al.*, 2009; Henry *et al.*, 2015). In this study, the *in vitro* SnRK1 activity was not directly affected by light intensity, but may have been modulated *in vivo* by changes in leaf T6P content, which correlated with its strong *in vitro* inhibition by T6P and the expression of well characterized SnRK1 downstream targets (**Fig. 2-3, 6**), which clearly responded to light and associated changes in T6P. However, there was less good correlation when analysing the overall set of SnRK1 target genes previously characterized in Arabidopsis (**Fig. 6, Table S2**). This may indicate that different subsets of genes could respond to SnRK1 in either a tissue and/or C₄ dependent manner. Glucose usually activates TOR, which generally acts antagonistically to SnRK1, to promote growth by triggering the down- and up-regulation of hundreds of genes involved in catabolism and anabolism in sink tissues (Xiong *et al.*, 2013; Tomé *et al.*, 2014; Baena-González and Hanson, 2017). In this study, we did not observe a response of TOR to LL or HL, indicating that this pathway might not play a critical role in the response to light intensity and sugar levels in C₄ source leaves, at least not with our experimental system over the timeframe we investigated (**Fig. 6, Table S2**). Although the ectopic overexpression of *AtTOR* improved rice photosynthesis and water use efficiency, especially under water limitation (Bakshi *et al.*, 2017), most studies conducted on Arabidopsis showed that the TOR signalling pathway plays a critical role in young developing sink tissues rather than in source leaves (Anderson *et al.*, 2005; Deprost *et al.*, 2005, 2007; Leiber *et al.*, 2010; Xiong *et al.*, 2013; Montané and Menand, 2013). This could explain why TOR was not activated by HL and glucose accumulation in the source leaves of *S. viridis*. In summary, the effects of light intensity and sugar levels on sugar signalling in C₄ source leaves differs from what has been previously reported for C₃ source leaves and sink tissues.

Several hypotheses may explain the unexpected sugar signalling responses we observed. The list of TOR and SnRK1 downstream targets used as references in our study were identified based on studies carried on Arabidopsis or transgenic mesophyll protoplasts over- or under-expressing SnRK1 (Baena-González and Sheen, 2008; Xiong *et al.*, 2013).. We used attached source C₄ monocot *S. viridis* leaves which differ from Arabidopsis C₃ dicots in their leaf anatomy and physiology (between mesophyll and bundle sheath cells) and light requirement. The set of SnRK1 downstream targets may differ between: (1) intact leaves and isolated protoplasts, (2) C₃ and C₄ mesophyll cells, and (3) bundle sheath and mesophyll cells in C₄ plants due to the contrasting partitioning of sucrose and starch biosynthesis in C₄ leaves (Lunn and Furbank, 1999).

The regulation of SnRK1 downstream targets in C₃ and C₄ species may also have different threshold sugar levels required to trigger sugar signalling responses. In C₄ maize sink tissue, for example, the SnRK1 Ki for inhibition by T6P was 50 µM (Nuccio *et al.*, 2015)

compared to 4-5 μM in Arabidopsis seedlings (Nunes *et al.*, 2013). According to our results using C_4 source leaves and additional data mining of experiments using C_3 Arabidopsis shoots, leaves or seedlings, the activation of the HXK-dependent pathway appears to require high sugar accumulation, irrespective of the species (Xiong *et al.*, 2013; Van Aken *et al.*, 2013; Li *et al.*, 2015a). On the other hand, the SnRK1 targets have been authenticated at physiological levels of sugar accumulation in response to low temperature and low nitrogen that induce sugar accumulation and in response to feeding sucrose at physiological levels (Zhang *et al.*, 2009; Nunes *et al.*, 2013). Genes regulated by glucose through the TOR pathway in Arabidopsis were identified after 2h of treatment with only 15 mM glucose (Xiong *et al.*, 2013). Hence, the unexpected sugar signalling responses we observed may reflect a systematic difference in the threshold of sugar sensitivity between different sugar sensors and/or between C_3 and C_4 tissues, which will be the focus of our future research.

Alternatively, the response of *S. viridis* C_4 leaves to LL and HL, and the resulting changes in sugar levels may have involved other sugar signalling pathways that have not yet been characterized in plants. Additionally, the response of C_4 source leaves to LL and HL may be predominantly triggered by light signalling pathways. Chloroplasts have been involved in plant responses to fluctuating light intensities through a process called “retrograde signalling”. Chloroplast retrograde signalling can alter the expression of various genes, especially genes involved in photosynthesis (Szechyńska-Hebda and Karpiński, 2013; Chan *et al.*, 2016). Changes in light intensity are also sensed by phytochrome light sensors through a shift in the ratio of red to far red light, which usually occurs under shading (Jiao *et al.*, 2007; Bae and Choi, 2008; Van Buskirk *et al.*, 2012; Xu *et al.*, 2015). Since C_4 source leaves have very high light requirements and rely on it to produce sugars in contrast to sink tissues, which rely on imported sugars to develop and grow, light signalling might override sugar signalling in *S. viridis* leaves.

Sugar versus light signalling pathways in source leaves of C_4 *S. viridis*

Although our experimental design does not allow us to separate light from sugar-related signalling responses, we attempted to interpret our results with data available in the literature. Consequently, we compared the effect of sugars and light on the expression of the downstream targets of HXK, TOR and SnRK1, between our experiments and similar experiments using *A. thaliana* (Xiong *et al.*, 2013; Van Aken *et al.*, 2013; Li *et al.*, 2015a). In *A. thaliana* plants treated with darkness or high light ($1000 \mu\text{mol m}^{-2} \text{s}^{-1}$), the expression of HXK downstream targets was affected, but not in a clear fashion. Most of the HXK-repressible targets were repressed under both darkness and high light. Additionally, those targets were not clearly affected by the addition of physiological levels of glucose (15 mM) or sucrose (1%) (Table S4, Fig. S7). Hence, in Arabidopsis, the expression of the key HXK

downstream targets seems to be affected by darkness and high light, but not by low levels of sugars as reported in studies in which these genes were originally identified. The discrepancy in the literature may be due to the relatively high (2-3% of sucrose or 50-300 mM of sucrose or glucose) level of sugars used to identify these genes (Jang and Sheen, 1994; Jang *et al.*, 1997; Zhou *et al.*, 1998; Sheen *et al.*, 1999; Xiao *et al.*, 2000; Moore *et al.*, 2003; Kunz *et al.*, 2014, 2015). Taken together these results indicate that HXK might be more responsive to light intensity than to physiologically-relevant changes in glucose levels and that the HXK-dependent pathway might require dramatic changes in glucose levels to be activated, both in C₃ and C₄ species. Hence, the unexpected induction of the HXK-dependent pathway we observed under LL and sugar depletion, is likely due to the effect of light rather than sugars. Similarly, the absence of the expected activation of the HXK-dependent pathway by HL and sugar accumulation in *S. viridis*, in contrast to initial reports using Arabidopsis fed with high sugar levels, is consistent with our re-analysis of the published datasets using low sugar concentrations. These results indicate that the absence of the activation of the HXK-dependent pathway we observed under HL is likely due to an insufficient change in sugar levels and/or the overriding effect of light signalling.

On the other hand, in re-analysed data, the expression of the key downstream targets of TOR and SnRK1 in Arabidopsis is more clearly and consistently affected by sugars, although they can also be regulated by light (**Table S4, Fig. S7**). These results indicate that in our experiments, the SnRK1 signalling pathway is more likely to be activated by sugar depletion under LL and repressed by sugar accumulation under HL than by the light intensity itself. We are currently using sugar sensing mutants to further investigate this hypothesis. Finally, TOR was not affected by changes in sugar levels or light intensity in our study, unlike observations using similar experiments in Arabidopsis, which indicates possible differences between species and/or source and sink tissues.

SUPPLEMENTARY DATA

Table S1: A_{net}/C_i , fluorescence and chlorophyll content parameters in light treated *S. viridis* leaves

Table S2: Number of key transcripts affected by light treatments in *S. viridis* leaves

Table S3: Mapman4 gene category enrichment in light treated *S. viridis* leaves

Table S4: Summary of the effect of darkness, high light, glucose and sucrose on the transcript levels of key sugar signalling targets in *A. thaliana*

Table S5: Log2 FC and classification of all transcripts DE expressed in light treated *S. viridis* leaves

Figure S1: Experimental design and phenotype of *S. viridis* plants after light treatments

Figure S2: Time for light treated *S. viridis* leaves to reach steady state at high irradiance

Figure S3: A_{net}/C_i curves of light treated *S. viridis* leaves at high irradiance

Figure S4: *In vitro* activity and content of key photosynthetic enzymes from light treated *S. viridis* leaves

Figure S5: Relative level of Fructose, Sucrose-6-P and Trehalose in light treated *S. viridis* leaves

Figure S6: Dynamic changes of the whole transcriptome and the full sets of TOR and SnRK1 predicted downstream targets in light treated *S. viridis* leaves

Figure S7: Effect of darkness, high light, glucose and sucrose on the transcript levels of our key sugar signalling targets in *A. thaliana*

ACKNOWLEDGEMENTS

We thank Fiona Koller, Bethanie Coleman and Samantha Prior for their technical assistance. This research was funded by the ARC Centre of Excellence for Translational Photosynthesis (CE140100015) awarded to Oula Ghannoum and Robert Furbank. Rothamsted Research receives strategic funding from the Biotechnological and Biological Sciences Research Council of the United Kingdom. We acknowledge support through the designing future wheat (DFW) strategic programme (BB/P016855/1).

FIGURE LEGENDS

Figure 1: Photosynthetic capacity of *S. viridis* plants is strongly impaired by low light while it is not affected by high light. Dynamic changes in photosynthetic rates (A, D and G), leaf conductance (B, E and H) and leaf internal CO₂ concentration (C, F and I) of Low Light (LL, 50 $\mu\text{mol}\cdot\text{m}^{-2}\cdot\text{s}^{-1}$), Medium Light (ML, 500 $\mu\text{mol}\cdot\text{m}^{-2}\cdot\text{s}^{-1}$, control) and High Light (HL, 1000 $\mu\text{mol}\cdot\text{m}^{-2}\cdot\text{s}^{-1}$) treated *S. viridis* plants provided with high light intensity (1000 $\mu\text{mol}\cdot\text{m}^{-2}\cdot\text{s}^{-1}$, 10% blue light) or growth light intensity (50, 500 or 1000 $\mu\text{mol}\cdot\text{m}^{-2}\cdot\text{s}^{-1}$, 10% blue light) and current ambient CO₂ reference concentration (400 ppm) for gas exchange measurements. For every time point, the midsection of the last fully expanded leaf was clamped to the gas exchange chamber and measurements were taken every minute for up to 1.5h after clamping. Here we present measurements taken 25 min after clamping (A-C) as well as when plants reached their maximum photosynthetic rates at steady state (D-I). All measurements were carried from morning to early afternoon on 3 to 5 different plants for each time point and treatment. Stars indicate statistical differences ($p < 0.05$) between the treated and control plants for each given time point.

Figure 2: Low light gradually reduces the levels of key sugars in the leaves of *S. viridis* while high light causes a strong and gradual build-up of those sugars over time. Dynamic changes in glucose (A), sucrose (B) and trehalose-6-P (C) content in fully expanded leaves of LL (50 $\mu\text{mol}\cdot\text{m}^{-2}\cdot\text{s}^{-1}$), ML (500 $\mu\text{mol}\cdot\text{m}^{-2}\cdot\text{s}^{-1}$) and HL (1000 $\mu\text{mol}\cdot\text{m}^{-2}\cdot\text{s}^{-1}$) treated *S. viridis* plants before and during treatment. Sugars were extracted from leaf blade samples collected from the midsection of the last fully expanded leaf at midday (6h after lights were turned on). Sugar levels were measured using semi-quantitative (LC-MS). Sugar levels are semi-quantitative, expressed relatively to Day 0 ML samples and normalized per fresh weight. For each treatment and time point the assays were carried on 4 independent biological replicates. Stars indicate statistical differences ($p < 0.05$) between the treated and control plants for each given time point.

Figure 3: SnRK1 *in vitro* activity of from *S. viridis* leaves is not significantly affected by low or high light treatment, but is reduced to about half in presence of T6P. Dynamic changes in total (A) and T6P inhibited (B) SnRK1 *in vitro* kinase activity from protein extracts of fully expanded *S. viridis* leaves treated with LL (50 $\mu\text{mol}\cdot\text{m}^{-2}\cdot\text{s}^{-1}$), ML (500 $\mu\text{mol}\cdot\text{m}^{-2}\cdot\text{s}^{-1}$) and HL (1000 $\mu\text{mol}\cdot\text{m}^{-2}\cdot\text{s}^{-1}$). For SnRK1 inhibition assays (B), 1 mM of exogenous T6P was added to the reaction. Kinase activities were normalised per amount of total proteins. For each treatment and time point the assays were carried on 4 independent

biological replicates. Stars indicate statistical differences ($p < 0.05$) between the treated and control plants for each given time point.

Figure 4: Low light downregulates >70 % of the photosynthetic gene transcripts expressed in *S. viridis* leaves, while high light has little to no effect on most of them.

Heatmap representing the dynamic changes in transcript levels of photosynthetic genes in *S. viridis* leaves treated with LL ($50 \mu\text{mol m}^{-2} \text{s}^{-1}$) and HL ($1000 \mu\text{mol m}^{-2} \text{s}^{-1}$) relative to ML ($500 \mu\text{mol m}^{-2} \text{s}^{-1}$, control) before (Day 0) and during treatment (Day 1, 2 and 4) using RNAseq. A total of 244 out of 301 detected photosynthetic transcripts were differentially expressed between all the conditions. For each treatment, analyses were carried on 3 independent biological replicates. We used cut-off values of at least 1CPM in at least 2 samples and a FDR of 0.05 for the differential expression analysis with DESeq2. Blue and yellow lines respectively represent a significant decrease or increase in transcript levels in the treatment compared to the control. Genes were classified based on their respective differential expression as follows (Fold Change compared to control): (Class -3, Highly repressed) $< -5 \text{ FC} < (\text{Class -2, Mildly repressed}) < -2 \text{ FC} < (\text{Class -1, Slightly repressed}) < 0 \text{ FC} = (\text{Class 0, Unaffected}) < (\text{Class 1, Slightly induced}) < 2 \text{ FC} < (\text{Class 2, Mildly induced}) < 5 \text{ FC} < (\text{Class 3, Highly induced})$.

Figure 5: Low light affects the transcript levels of most of the key sugar sensors and trehalose pathway genes expressed in *S. viridis* leaves, while high light has a smaller but antagonist effect.

Heatmap representing the dynamic changes in transcript levels of sugar sensors (HXK, TOR complex and SnRK1 complex) and trehalose pathway (TPS, TPP and TRE) genes in leaves treated with LL ($50 \mu\text{mol m}^{-2} \text{s}^{-1}$) and HL ($1000 \mu\text{mol m}^{-2} \text{s}^{-1}$) relative to ML ($500 \mu\text{mol m}^{-2} \text{s}^{-1}$, control) before (Day 0) and during treatment (Day 1, 2 and 4) using RNAseq. A total of 22 out of 52 sugar signalling transcripts were differentially regulated between all the treatments. For each treatment, analyses were carried on 3 independent biological replicates. We used cut-off values of at least 1CPM in at least 2 samples and a FDR of 0.05 for the differential expression analysis with DESeq2. Blue and yellow lines respectively represent a significant decrease or increase in transcript levels in the treatment compared to the control. Genes were classified based on their respective differential expression as follows (Fold Change compared to control): (Class -3, Highly repressed) $< -5 \text{ FC} < (\text{Class -2, Mildly repressed}) < -2 \text{ FC} < (\text{Class -1, Slightly repressed}) < 0 \text{ FC} = (\text{Class 0, Unaffected}) < (\text{Class 1, Slightly induced}) < 2 \text{ FC} < (\text{Class 2, Mildly induced}) < 5 \text{ FC} < (\text{Class 3, Highly induced})$.

Figure 6: Light treatment had a clear impact on the expression of key HXK and SnRK downstream targets, but no effect on key TOR downstream targets in mature C₄ *S. viridis* leaves. Heatmaps representing the dynamic changes in transcript levels of key downstream targets of HXK (A), TOR (B) and SnRK1 (C) in mature *S. viridis* leaves treated with LL (50 $\mu\text{mol m}^{-2} \text{s}^{-1}$) and HL (1000 $\mu\text{mol m}^{-2} \text{s}^{-1}$) relative to ML (500 $\mu\text{mol m}^{-2} \text{s}^{-1}$, control) before (Day 0) and during treatment (Day 1, 2 and 4). For each treatment, analyses were carried on 3 independent biological replicates. We used cut-off values of at least 1CPM in at least 2 samples and a FDR of 0.05 for the differential expression analysis with DESeq2. Blue and yellow lines respectively represent a significant decrease or increase in transcript levels in the treatment compared to the control. Genes were classified based on their respective differential expression as follows (Fold Change compared to control): (Class -3, Highly repressed) < -5 FC < (Class -2, Mildly repressed) < -2 FC < (Class -1, Slightly repressed) < 0 FC = (Class 0, Unaffected) < (Class 1, Slightly induced) < 2 FC < (Class 2, Mildly induced) < 5 FC < (Class 3, Highly induced).

Accepted Manuscript

REFERENCES

- Van Aken O, Zhang B, Law S, Narsai R, Whelan J.** 2013. AtWRKY40 and AtWRKY63 modulate the expression of stress-responsive nuclear genes encoding mitochondrial and chloroplast proteins. *Plant Physiology* **162**, 254–271.
- Anderson GH, Veit B, Hanson MR.** 2005. The Arabidopsis AtRaptor genes are essential for post-embryonic plant growth. *BMC biology* **3**, 12.
- Andrès C, Agne B, Kessler F.** 2010. The TOC complex: Preprotein gateway to the chloroplast. *Biochimica et Biophysica Acta (BBA) - Molecular Cell Research* **1803**, 715–723.
- Bae G, Choi G.** 2008. Decoding of light signals by plant phytochromes and their interacting proteins. *Annual Review of Plant Biology* **59**, 281–311.
- Baena-González E.** 2010. Energy signaling in the regulation of gene expression during stress. *Molecular plant* **3**, 300–313.
- Baena-González E, Hanson J.** 2017. Shaping plant development through the SnRK1–TOR metabolic regulators. *Current Opinion in Plant Biology* **35**, 152–157.
- Baena-Gonzalez E, Rolland F, Thevelein JM, Sheen J.** 2007. A central integrator of transcription networks in plant stress and energy signalling. *Nature* **448**, 938–942.
- Baena-González E, Sheen J.** 2008. Convergent energy and stress signaling. *Trends in Plant Science* **13**, 474–482.
- Bakshi A, Moin M, Kumar MU, Reddy ABM, Ren M, Datla R, Siddiq EA, Kirti PB.** 2017. Ectopic expression of *Arabidopsis Target of Rapamycin (AtTOR)* improves water-use efficiency and yield potential in rice. *Scientific Reports* **7**, 42835.
- Bennetzen JL, Schmutz J, Wang H, et al.** 2012. Reference genome sequence of the model plant *Setaria*. *Nature Biotechnology* **30**, 555–561.
- Bläsing O, Gibon Y, Günther M, Hohne M, Morcuende R, Osuna D, Thimm O, Usadel B, Scheible W-R, Stitt M.** 2005. Sugars and circadian regulation make major contributions to the global regulation of diurnal gene expression in *Arabidopsis*. *The Plant Cell* **17**, 3257–3281.
- Bolger AM, Lohse M, Usadel B.** 2014. Trimmomatic: a flexible trimmer for Illumina sequence data. *Bioinformatics (Oxford, England)* **30**, 2114–20.
- Bracher A, Whitney SM, Hartl FU, Hayer-Hartl M.** 2017. Biogenesis and metabolic maintenance of Rubisco. *Annual Review of Plant Biology* **68**, 29–60.
- Brauner K, Stutz S, Paul M, Heyer AG.** 2015. Measuring whole plant CO₂ exchange with the environment reveals opposing effects of the gin2–1 mutation in shoots and roots of *Arabidopsis thaliana*. *Plant Signaling & Behavior* **10**, e973822.
- Browning KS, Bailey-Serres J.** 2015. Mechanism of cytoplasmic mRNA translation. *The arabidopsis book* **13**, e0176.

- Brutnell TP, Wang L, Swartwood K, Goldschmidt A, Jackson D, Zhu X-G, Kellogg E, Van Eck J.** 2010. *Setaria viridis*: A model for C₄ photosynthesis. *The Plant Cell* **22**, 2537–2544.
- Van Buskirk EK, Decker P V, Chen M.** 2012. Photobodies in light signaling. *Plant physiology* **158**, 52–60.
- Caldana C, Li Y, Leisse A, Zhang Y, Bartholomaeus L, Fernie AR, Willmitzer L, Giavalisco P.** 2013. Systemic analysis of inducible target of rapamycin mutants reveal a general metabolic switch controlling growth in *Arabidopsis thaliana*. *The Plant journal : for cell and molecular biology* **73**, 897–909.
- Chan KX, Phua SY, Crisp P, McQuinn R, Pogson BJ.** 2016. Learning the languages of the chloroplast: retrograde signaling and beyond. *Annual Review of Plant Biology* **67**, 25–53.
- Cho YH, Hong JW, Kim EC, Yoo SD.** 2012. Regulatory functions of SnRK1 in stress-responsive gene expression and in plant growth and development. *Plant physiology* **158**, 1955–1964.
- Cho JI, Ryoo N, Eom JS, et al.** 2008. Role of the rice hexokinases OsHXK5 and OsHXK6 as glucose sensors. *Plant Physiology* **149**, 745–759.
- Dai N, Schaffer A, Petreikov M, Shahak Y, Giller Y, Ratner K, Levine A, Granot D.** 1999. Overexpression of *Arabidopsis* hexokinase in tomato plants inhibits growth, reduces photosynthesis, and induces rapid senescence. *The Plant Cell* **11**, 1253–1266.
- Deprost D, Truong H-N, Robaglia C, Meyer C.** 2005. An *Arabidopsis* homolog of RAPTOR/KOG1 is essential for early embryo development. *Biochemical and biophysical research communications* **326**, 844–850.
- Deprost D, Yao L, Sormani R, Moreau M, Leterreux G, Nicolai M, Bedu M, Robaglia C, Meyer C.** 2007. The *Arabidopsis* TOR kinase links plant growth, yield, stress resistance and mRNA translation. *EMBO reports* **8**, 864–870.
- Ding Z, Zhang Y, Xiao Y, et al.** 2016. Transcriptome response of cassava leaves under natural shade. *Scientific reports* **6**, 31673.
- Dobrenel T, Marchive C, Sormani R, Moreau M, Mozzo M, Montané M-H, Menand B, Robaglia C, Meyer C.** 2011. Regulation of plant growth and metabolism by the TOR kinase. *Biochemical Society transactions* **39**, 477–481.
- Dong P, Xiong F, Que Y, Wang K, Yu L, Li Z, Ren M.** 2015. Expression profiling and functional analysis reveals that TOR is a key player in regulating photosynthesis and phytohormone signaling pathways in *Arabidopsis*. *Frontiers in plant science* **6**, 677.
- Figuroa CM, Lunn JE.** 2016. A tale of two sugars: trehalose 6-phosphate and sucrose. *Plant Physiology* **172**, 7–27.
- Flores-Pérez Ú, Jarvis P.** 2013. Molecular chaperone involvement in chloroplast protein import. *Biochimica et Biophysica Acta (BBA) - Molecular Cell Research* **1833**, 332–340.

- Ghannoum O, Evans JR, von Caemmerer S.** 2011. Chapter 8 - Nitrogen and water use efficiency of C₄ plants. In: Raghavendra AS, In: Sage RF, eds. C₄ photosynthesis and related CO₂ concentrating mechanisms. Springer Netherlands, 129–146.
- Goldschmidt EE, Huber SC.** 1992. Regulation of photosynthesis by end-product accumulation in leaves of plants storing starch, sucrose, and hexose sugars. *Plant physiology* **99**, 1443–1448.
- Gong W, Qi P, Du J, et al.** 2014. Transcriptome analysis of shade-induced inhibition on leaf size in relay intercropped soybean. *PLoS ONE* **9**, e98465.
- Griffiths CA, Paul MJ, Foyer CH.** 2016. Metabolite transport and associated sugar signalling systems underpinning source/sink interactions. *Biochimica et Biophysica Acta (BBA) - Bioenergetics* **1857**, 1715–1725.
- Hatch MD.** 1987. C₄ photosynthesis: a unique blend of modified biochemistry, anatomy and ultrastructure. *Biochimica et Biophysica Acta (BBA) - Reviews on Bioenergetics* **895**, 81–106.
- Henriques R, Bögre L, Horváth B, Magyar Z.** 2014. Balancing act: matching growth with environment by the TOR signalling pathway. *Journal of experimental botany* **65**, 2691–2701.
- Henry C, Bledsoe SW, Griffiths CA, Kollman A, Paul MJ, Sakr S, Lagrimini LM.** 2015. Differential role for trehalose metabolism in salt-stressed maize. *Plant Physiology* **169**, 1072–1089.
- Jang JC, Leon P, Zhou L, Sheen J.** 1997. Hexokinase as a sugar sensor in higher plants. *The Plant Cell* **9**, 5–19.
- Jang JC, Sheen J.** 1994. Sugar sensing in higher plants. *The Plant cell* **6**, 1665–1679.
- Jiao Y, Lau OS, Deng XW.** 2007. Light-regulated transcriptional networks in higher plants. *Nature Reviews Genetics* **8**, 217–230.
- John CR, Smith-Unna RD, Woodfield H, Covshoff S, Hibberd JM.** 2014. Evolutionary convergence of cell-specific gene expression in independent lineages of C₄ grasses. *Plant physiology* **165**, 62–75.
- Kalt-Torres W, Kerr PS, Usuda H, Huber SC.** 1987. Diurnal changes in maize leaf photosynthesis : I. Carbon exchange rate, assimilate export rate, and enzyme activities. *Plant physiology* **83**, 283–288.
- Karki S, Rizal G, Quick W.** 2013. Improvement of photosynthesis in rice (*Oryza sativa* L.) by inserting the C₄ pathway. *Rice* **6**, 28.
- Kelly G, David-Schwartz R, Sade N, Moshelion M, Levi A, Alchanatis V, Granot D.** 2012. The pitfalls of transgenic selection and new roles of *AtHXK1*: a high level of *AtHXK1* expression uncouples hexokinase1-dependent sugar signaling from exogenous sugar. *Plant physiology* **159**, 47–51.
- Kelly G, Moshelion M, David-Schwartz R, Halperin O, Wallach R, Attia Z, Belausov E, Granot D.** 2013. Hexokinase mediates stomatal closure. *The Plant Journal* **75**, 977–988.

- Kelly G, Sade N, Attia Z, Secchi F, Zwieniecki M, Holbrook NM, Levi A, Alchanatis V, Moshelion M, Granot D.** 2014. Relationship between hexokinase and the aquaporin PIP1 in the regulation of photosynthesis and plant growth. *PLoS ONE* **9**, e87888.
- Kikuchi S, Bedard J, Hirano M, Hirabayashi Y, Oishi M, Imai M, Takase M, Ide T, Nakai M.** 2013. Uncovering the protein translocon at the chloroplast inner envelope membrane. *Science* **339**, 571–574.
- Krapp A, Stitt M.** 1995. An evaluation of direct and indirect mechanisms for the ‘sink-regulation’ of photosynthesis in spinach: Changes in gas exchange, carbohydrates, metabolites, enzyme activities and steady-state transcript levels after cold-girdling source leaves. *Planta* **195**, 313–323.
- Kretschmar T, Pelayo MAF, Trijatmiko KR, et al.** 2015. A trehalose-6-phosphate phosphatase enhances anaerobic germination tolerance in rice. *Nature Plants* **1**, 15124.
- Krishna P, Gloor G.** 2001. The Hsp90 family of proteins in *Arabidopsis thaliana*. *Cell stress & chaperones* **6**, 238–46.
- Kunz S, Gardeström P, Pesquet E, Kleczkowski LA.** 2015. Hexokinase 1 is required for glucose-induced repression of bZIP63, At5g22920, and BT2 in *Arabidopsis*. *Frontiers in plant science* **6**, 525.
- Kunz S, Pesquet E, Kleczkowski LA.** 2014. Functional dissection of sugar signals affecting gene expression in *Arabidopsis thaliana*. *PLoS ONE* **9**, e100312.
- Langmead B, Salzberg SL.** 2012. Fast gapped-read alignment with Bowtie 2. *Nature Methods* **9**, 357–359.
- Leegood RC.** 2000. Transport During C4 Photosynthesis. In: Leegood Sharkey, T.D., von Caemmerer, S. RC, ed. *Photosynthesis. Advances in Photosynthesis and Respiration*. Dordrecht: Springer, 459–469.
- Leiber R-M, John F, Verhertbruggen Y, Diet A, Knox JP, Ringli C.** 2010. The TOR pathway modulates the structure of cell walls in *Arabidopsis*. *The Plant cell* **22**, 1898–908.
- Li Y, Andrade J.** 2017. DEApp: an interactive web interface for differential expression analysis of next generation sequence data. *Source code for biology and medicine* **12**, 2.
- Li P, Brutnell TP.** 2011. *Setaria viridis* and *Setaria italica*, model genetic systems for the Panicoid grasses. *Journal of experimental botany* **62**, 3031–3037.
- Li Y, Mukherjee I, Thum KE, Tanurdzic M, Katari MS, Obertello M, Edwards MB, McCombie WR, Martienssen RA, Coruzzi GM.** 2015a. The histone methyltransferase SDG8 mediates the epigenetic modification of light and carbon responsive genes in plants. *Genome Biology* **16**, 79.
- Li L, Sheen J.** 2016. Dynamic and diverse sugar signaling. *Current opinion in plant biology* **33**, 116–125.
- Li L, Song Y, Wang K, Dong P, Zhang X, Li F, Li Z, Ren M.** 2015b. TOR-inhibitor

insensitive-1 (TRIN1) regulates cotyledons greening in Arabidopsis. *Frontiers in plant science* **6**, 861.

Lohse M, Nagel A, Herter T, May P, Schroda M, Zrenner R, Tohge T, Fernie AR, Stitt M, Usadel B. 2014. Mercator: a fast and simple web server for genome scale functional annotation of plant sequence data. *Plant, Cell & Environment* **37**, 1250–1258.

Love MI, Huber W, Anders S. 2014. Moderated estimation of fold change and dispersion for RNA-seq data with DESeq2. *Genome Biology* **15**.

Lunn JE, Furbank RT. 1997. Localisation of sucrose-phosphate synthase and starch in leaves of C₄ plants. *Planta* **202**, 106–111.

Lunn JE, Furbank RT. 1999. Sucrose biosynthesis in C₄ plants. *New Phytologist* **143**, 221–237.

Martínez-Barajas E, Delatte T, Schluemann H, de Jong GJ, Somsen GW, Nunes C, Primavesi LF, Coello P, Mitchell R a C, Paul MJ. 2011. Wheat grain development is characterized by remarkable trehalose 6-phosphate accumulation pregrain filling: tissue distribution and relationship to SNF1-related protein kinase1 activity. *Plant physiology* **156**, 373–381.

Merchante C, Stepanova AN, Alonso JM. 2017. Translation regulation in plants: an interesting past, an exciting present and a promising future. *The Plant Journal* **90**, 628–653.

Montané M-H, Menand B. 2013. ATP-competitive mTOR kinase inhibitors delay plant growth by triggering early differentiation of meristematic cells but no developmental patterning change. *Journal of experimental botany* **64**, 4361–474.

Moore B, Zhou L, Rolland F, Hall Q, Cheng W-H, Liu Y-X, Hwang I, Jones T, Sheen J. 2003. Role of the Arabidopsis glucose sensor HXK1 in nutrient, light, and hormonal signaling. *Science* **300**, 332–336.

Nakai M. 2015. The TIC complex uncovered: The alternative view on the molecular mechanism of protein translocation across the inner envelope membrane of chloroplasts. *Biochimica et Biophysica Acta (BBA) - Bioenergetics* **1847**, 957–967.

Nishimura K, Ogawa T, Ashida H, Yokota A. 2008. Molecular mechanisms of RuBisCO biosynthesis in higher plants. *Plant Biotechnology* **25**, 285–290.

Nuccio ML, Wu J, Mowers R, et al. 2015. Expression of trehalose-6-phosphate phosphatase in maize ears improves yield in well-watered and drought conditions. *Nature Biotechnology* **33**, 862–869.

Nukarinen E, Nägele T, Pedrotti L, et al. 2016. Quantitative phosphoproteomics reveals the role of the AMPK plant ortholog SnRK1 as a metabolic master regulator under energy deprivation. *Scientific Reports* **6**, 31697.

Nunes C, O'Hara LE, Primavesi LF, Delatte TL, Schluemann H, Somsen GW, Silva AB, Feveireiro PS, Wingler A, Paul MJ. 2013. The trehalose 6-phosphate/SnRK1 signaling

pathway primes growth recovery following relief of sink limitation. *Plant physiology* **162**, 1720–1732.

Oszvald M, Primavesi LF, Griffiths CA, Cohn J, Basu S, Nuccio ML, Paul MJ. 2018.

Trehalose 6-phosphate regulates photosynthesis and assimilate partitioning in reproductive tissue. *Plant Physiology* **176**, 2623–2638.

Pant SR, Irigoyen S, Doust AN, Scholthof K-BG, Mandadi KK. 2016. Setaria: A food crop and translational research model for C₄ grasses. *Frontiers in Plant Science* **7**, 1885.

Paul MJ, Foyer CH. 2001. Sink regulation of photosynthesis. *Journal of Experimental Botany* **52**, 1383–1400.

Paul MJ, Pellny TK. 2003. Carbon metabolite feedback regulation of leaf photosynthesis and development. *Journal of Experimental Botany* **54**, 539–547.

Pellny TK, Ghannoum O, Conroy JP, Schluempmann H, Smeekens S, Andralojc J, Krause KP, Goddijn O, Paul MJ. 2004. Genetic modification of photosynthesis with *E. coli* genes for trehalose synthesis. *Plant Biotechnology Journal* **2**, 71–82.

Porra RJ, Thompson WA, Kriedemann PE. 1989. Determination of accurate extinction coefficients and simultaneous equations for assaying chlorophylls a and b extracted with four different solvents: verification of the concentration of chlorophyll standards by atomic absorption spectroscopy. *Biochimica et Biophysica Acta* **975**, 384–394.

R Core Team. 2016. R: A language and environment for statistical computing.

Ramon M, Rolland F. 2007. Plant development: introducing trehalose metabolism. *Trends in Plant Science* **12**, 185–188.

Rexin D, Meyer C, Robaglia C, Veit B. 2015. TOR signalling in plants. *The Biochemical journal* **470**, 1–14.

Roberts A, Pachter L. 2013. Streaming fragment assignment for real-time analysis of sequencing experiments. *Nature methods* **10**, 71–3.

Rolland F, Baena-Gonzalez E, Sheen J. 2006. Sugar sensing and signaling in plants: conserved and novel mechanisms. *Annual review of plant biology* **57**, 675–709.

RStudio Team. 2015. RStudio: Integrated Development for R.

Sage RF, Percy RW. 2000. The physiological ecology of C₄ photosynthesis. Springer, Dordrecht, 497–532.

Sage RF, Sage TL, Kocacinar F. 2012. Photorespiration and the Evolution of C₄ Photosynthesis.

Sebastian J, Wong MK, Tang E, et al. 2014. Methods to promote germination of dormant *Setaria viridis* seeds. *PLoS ONE* **9**, e95109.

Sharwood RE, Ghannoum O, Whitney SM. 2016a. Prospects for improving CO₂ fixation in C₃-crops through understanding C₄-Rubisco biogenesis and catalytic diversity. *Current Opinion in Plant Biology* **31**, 135–142.

- Sharwood RE, Sonawane B V, Ghannoum O.** 2014. Photosynthetic flexibility in maize exposed to salinity and shade. *Journal of experimental botany* **65**, 3715–3724.
- Sharwood RE, Sonawane B V, Ghannoum O, Whitney SM.** 2016b. Improved analysis of C₄ and C₃ photosynthesis via refined *in vitro* assays of their carbon fixation biochemistry. *Journal of experimental botany* **67**, 3137–3148.
- Sheen J.** 1990. Metabolic repression of transcription in higher plants. *The Plant cell* **2**, 1027–1038.
- Sheen J, Zhou L, Jang J-C.** 1999. Sugars as signaling molecules. *Current Opinion in Plant Biology* **2**, 410–418.
- Sung DY, Vierling E, Guy CL.** 2001. Comprehensive expression profile analysis of the Arabidopsis Hsp70 gene family. *Plant physiology* **126**, 789–800.
- Szechyńska-Hebda M, Karpiński S.** 2013. Light intensity-dependent retrograde signalling in higher plants. *Journal of Plant Physiology* **170**, 1501–1516.
- Thimm O, Bläsing O, Gibon Y, Nagel A, Meyer S, Krüger P, Selbig J, Müller L a., Rhee SY, Stitt M.** 2004. Mapman: a User-Driven Tool To Display Genomics Data Sets Onto Diagrams of Metabolic Pathways and Other Biological Processes. *The Plant Journal* **37**, 914–939.
- Tomé F, Nägele T, Adamo M, et al.** 2014. The low energy signaling network. *Frontiers in plant science* **5**, 353.
- Trösch R, Mühlhaus T, Schroda M, Willmund F.** 2015. ATP-dependent molecular chaperones in plastids — More complex than expected. *BBA - Bioenergetics* **1847**, 872–888.
- Usuda H, Edwards GE.** 1984. Is photosynthesis during the induction period in maize limited by the availability of intercellular carbon dioxide? *Plant Science Letters* **37**, 41–45.
- Usuda H, Kalt-Torres W, Kerr PS, Huber SC.** 1987. Diurnal changes in maize leaf photosynthesis : II. Levels of metabolic intermediates of sucrose synthesis and the regulatory metabolite fructose 2,6-bisphosphate. *Plant physiology* **83**, 289–293.
- Usuda H, Ku MSB, Edwards GE.** 1985. Influence of light intensity during growth on photosynthesis and activity of several key photosynthetic enzymes in a C₄ plant (*Zea mays*). *Physiologia Plantarum* **63**, 65–70.
- Wang P, Vlad D, Langdale JA.** 2016. Finding the genes to build C₄ rice. *Current Opinion in Plant Biology* **31**, 44–50.
- Watson-Lazowski A, Papanicolaou A, Sharwood R, Ghannoum O.** 2018. Investigating the NAD-ME biochemical pathway within C₄ grasses using transcript and amino acid variation in C₄ photosynthetic genes. *Photosynthesis research*.
- Xiao W, Sheen J, Jang JC.** 2000. The role of hexokinase in plant sugar signal transduction and growth and development. *Plant Molecular Biology* **44**, 451–461.
- Xiong Y, McCormack M, Li L, Hall Q, Xiang C, Sheen J.** 2013. Glucose-TOR signalling

reprograms the transcriptome and activates meristems. *Nature* **496**, 181–186.

Xiong Y, Sheen J. 2015. Novel links in the plant TOR kinase signaling network. *Current opinion in plant biology* **28**, 83–91.

Xiong F, Zhang R, Meng Z, Deng K, Que Y, Zhuo F, Feng L, Guo S, Datla R, Ren M. 2017. Brassinosteroid Insensitive 2 (BIN2) acts as a downstream effector of the Target of Rapamycin (TOR) signaling pathway to regulate photoautotrophic growth in Arabidopsis. *New Phytologist* **213**, 233–249.

Xu X, Paik I, Zhu L, Huq E. 2015. Illuminating progress in phytochrome-mediated light signaling pathways. *Trends in plant science* **20**, 641–650.

Zhang Y, Primavesi LF, Jhurrea D, Andralojc PJ, Mitchell RAC, Powers SJ, Schluepmann H, Delatte T, Wingler A, Paul MJ. 2009. Inhibition of SNF1-related protein kinase1 activity and regulation of metabolic pathways by trehalose-6-phosphate. *Plant Physiology* **149**, 1860–1871.

Zhou L, Jang JC, Jones TL, Sheen J. 1998. Glucose and ethylene signal transduction crosstalk revealed by an Arabidopsis glucose-insensitive mutant. *Proceedings of the National Academy of Sciences of the United States of America* **95**, 10294–10299.

Accepted Manuscript

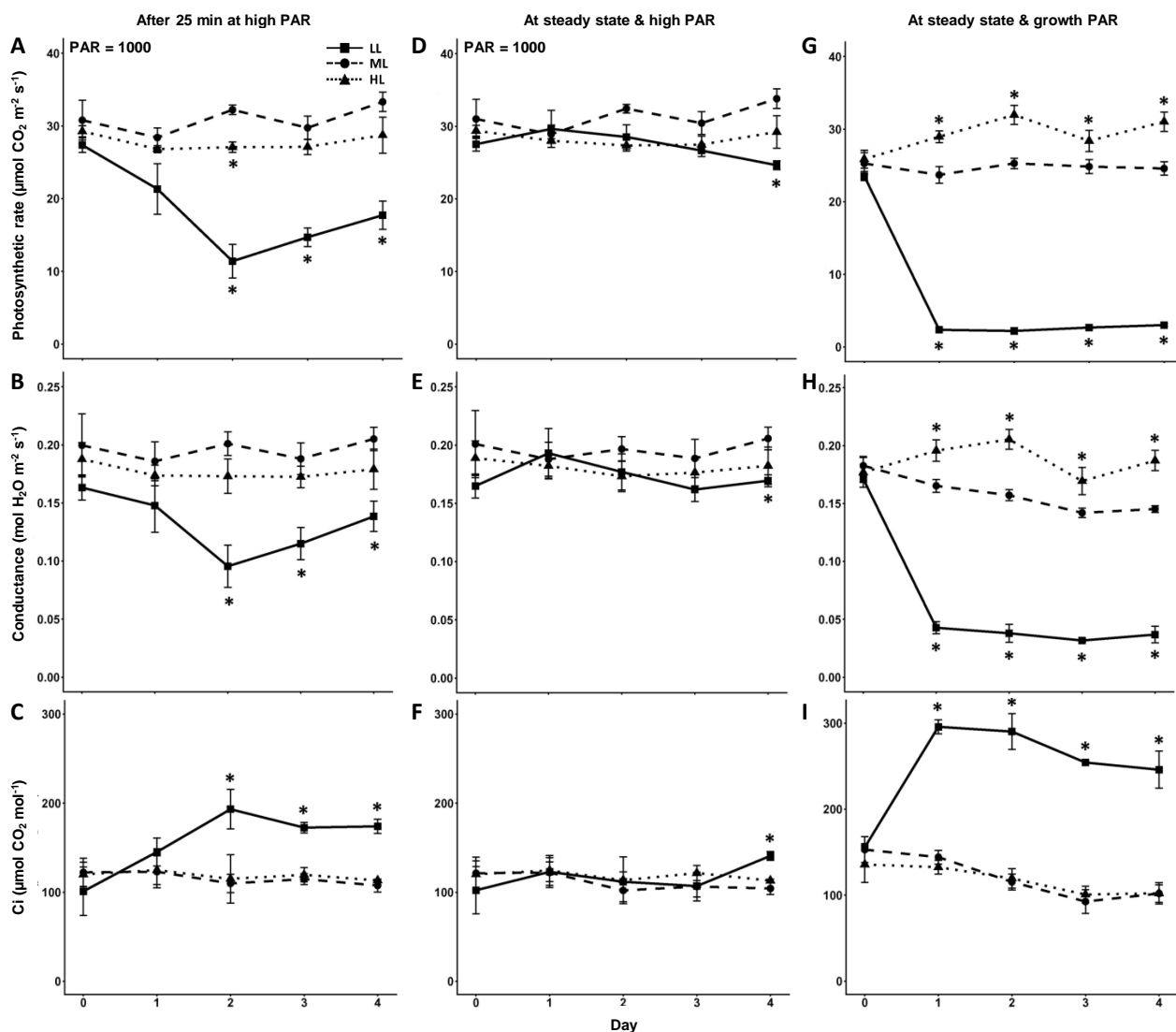


Figure 1: Photosynthetic capacity of *S. viridis* plants is strongly impaired by low light while it is not affected by high light. Dynamic changes in photosynthetic rates (A, D and G), leaf conductance (B, E and H) and leaf internal CO₂ concentration (C, F and I) of Low Light (LL, 50 $\mu\text{mol.m}^{-2}.\text{s}^{-1}$), Medium Light (ML, 500 $\mu\text{mol.m}^{-2}.\text{s}^{-1}$, control) and High Light (HL, 1000 $\mu\text{mol.m}^{-2}.\text{s}^{-1}$) treated *S. viridis* plants provided with high light intensity (1000 $\mu\text{mol.m}^{-2}.\text{s}^{-1}$, 10% blue light) or growth light intensity (50, 500 or 1000 $\mu\text{mol.m}^{-2}.\text{s}^{-1}$, 10% blue light) and ambient CO₂ reference concentration (400 ppm) for gas exchange measurements. For every time point, the midsection of the last fully expanded leaf was clamped to the gas exchange chamber and measurements were taken every minute for up to 1.5h after clamping. Here we present measurements taken 25 min after clamping (A - C) as well as when plants reached their maximum photosynthetic rates at steady state (D-I). All measurements were carried from morning to early afternoon on 3 to 5 different plants for each time point and treatment. Stars indicate statistical differences ($p < 0.05$) between the treated and control plants for each given time point.

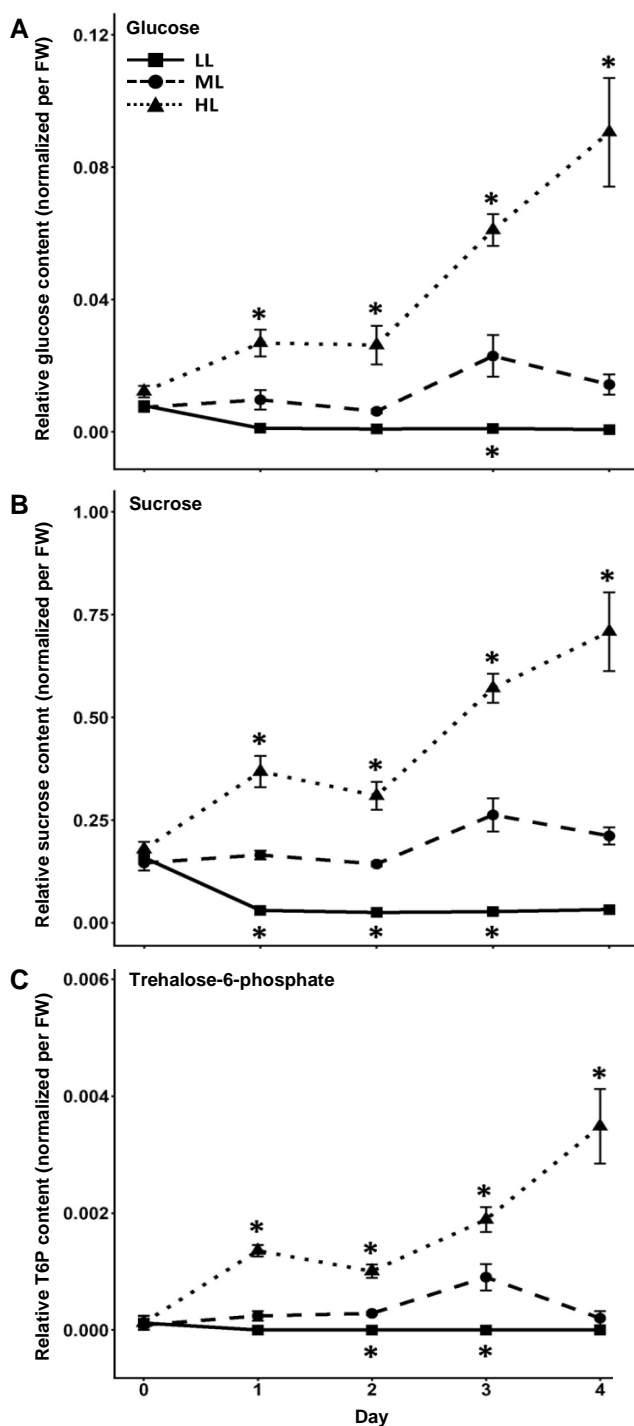


Figure 2: Low light gradually reduces the key sugar levels in the leaves of *S. viridis* while high light causes a strong and gradual build-up of those sugars over time. Dynamic changes in glucose (A), sucrose (B) and trehalose-6-P (C) content in fully expanded leaves of LL ($50 \mu\text{mol.m}^{-2}.\text{s}^{-1}$), ML ($500 \mu\text{mol.m}^{-2}.\text{s}^{-1}$) and HL ($1000 \mu\text{mol.m}^{-2}.\text{s}^{-1}$) treated *S. viridis* plants before and during treatment. Sugars were extracted from leaf blade samples collected from the midsection of the last fully expanded leaf at midday (6h after lights were turned on). Sugar levels were measured using semi-quantitative (LC-MS). Sugar levels are semi-quantitative, expressed relatively to Day 0 ML samples and normalized per fresh weight. For each treatment and time point the assays were carried on 4 independent biological replicates. Stars indicate statistical differences ($p < 0.05$) between the treated and control plants for each given time point.

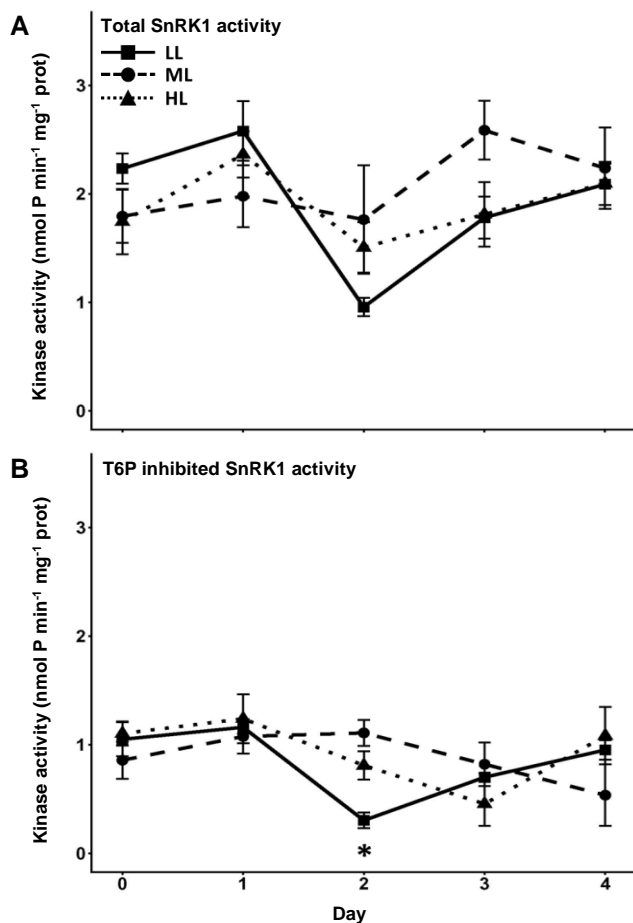


Figure 3: SnRK1 *in vitro* activity of from *S. viridis* leaves is not significantly affected by low or high light treatment, but is reduced to about half in presence of T6P. Dynamic changes in total (A) and T6P inhibited (B) SnRK1 *in vitro* kinase activity from protein extracts of fully expanded *S. viridis* leaves treated with LL ($50 \mu\text{mol.m}^{-2}.\text{s}^{-1}$), ML ($500 \mu\text{mol.m}^{-2}.\text{s}^{-1}$) and HL ($1000 \mu\text{mol.m}^{-2}.\text{s}^{-1}$). For SnRK1 inhibition assays (B), 1 mM of exogenous T6P was added to the reaction. Kinase activities were normalised per amount of total proteins. For each treatment and time point the assays were carried on 4 independent biological replicates. Stars indicate statistical differences ($p < 0.05$) between the treated and control plants for each given time point.

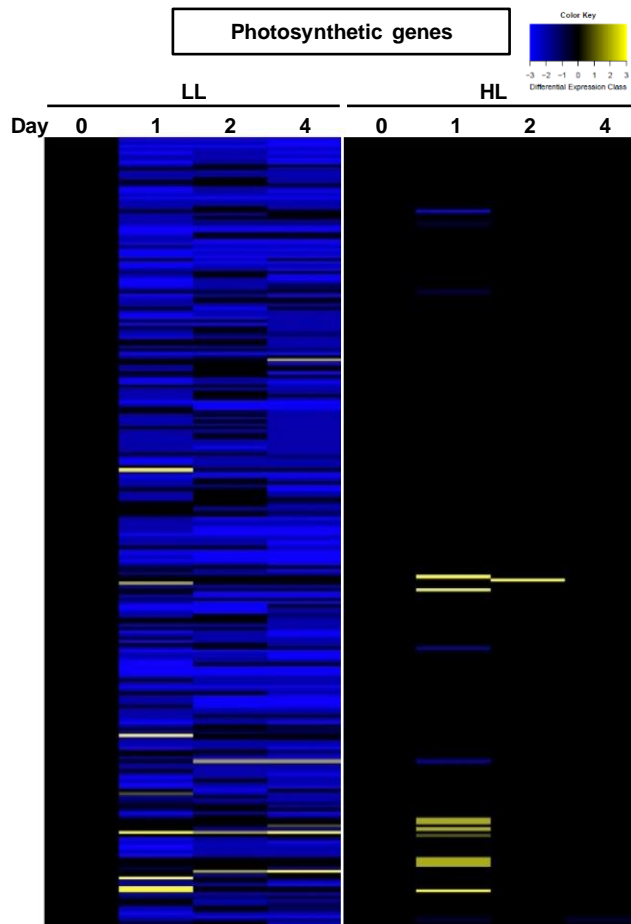


Figure 4: Low light downregulates >70 % of the photosynthetic gene transcripts expressed in *S. viridis* leaves, while high light has little to no effect on most of them. Heatmap representing the dynamic changes in transcript levels of photosynthetic genes in *S. viridis* leaves treated with LL (50 $\mu\text{mol}\cdot\text{m}^{-2}\cdot\text{s}^{-1}$) and HL (1000 $\mu\text{mol}\cdot\text{m}^{-2}\cdot\text{s}^{-1}$) relative to ML (500 $\mu\text{mol}\cdot\text{m}^{-2}\cdot\text{s}^{-1}$, control) before (Day 0) and during treatment (Day 1, 2 and 4) using RNAseq. A total of 244 out of 301 photosynthetic detected transcripts were differentially expressed between all the conditions. For each treatment, analyses were carried on 3 independent biological replicates. We used cut-off values of at least 1CPM in at least 2 samples and a FDR of 0.05 for the differential expression analysis with DESeq2. Blue and yellow lines respectively represent a significant decrease or increase in transcript levels in the treatment compared to the control. Genes were classified based on their respective differential expression as follows (Fold Change compared to control): (Class -3, Highly repressed) < -5 FC < (Class -2, Mildly repressed) < -2 FC < (Class -1, Slightly repressed) < 0 FC = (Class 0, Unaffected) < (Class 1, Slightly induced) < 2 FC < (Class 2, Mildly induced) < 5 FC < (Class 3, Highly induced).

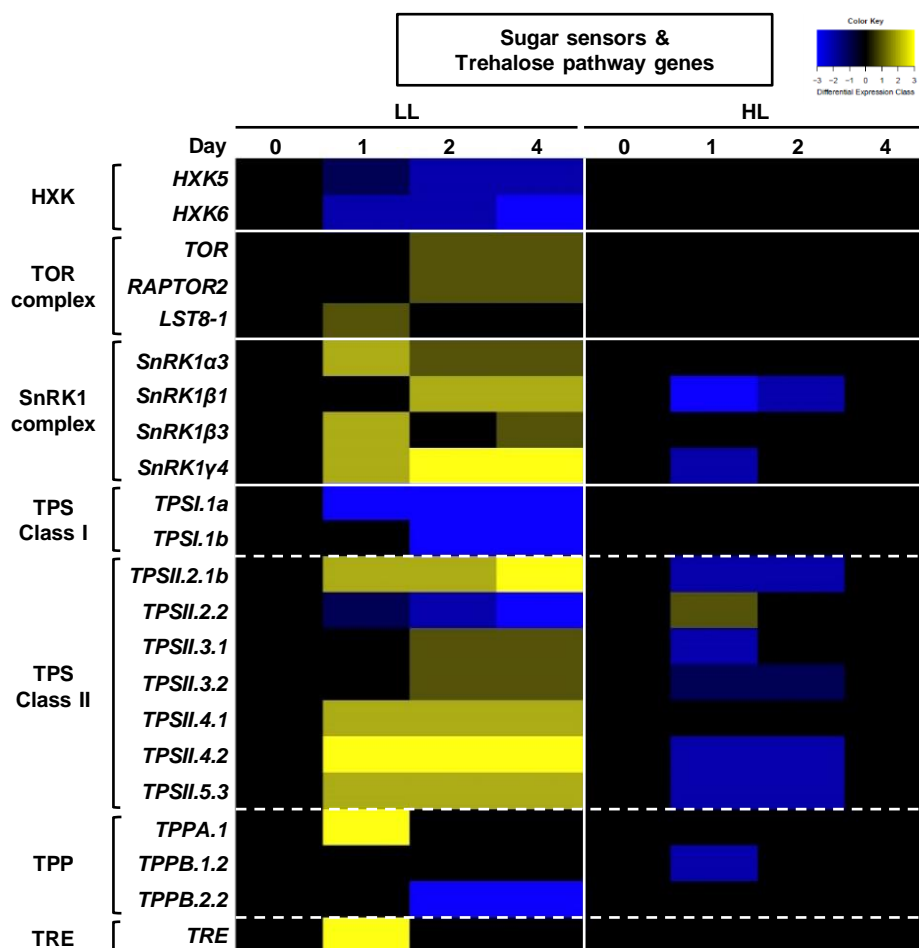


Figure 5: Low light affects the transcript levels of most of the key sugar sensors and trehalose pathway genes expressed in *S. viridis* leaves, while high light has a smaller but antagonist effect. Heatmap representing the dynamic changes in transcript levels of sugar sensors (HXK, TOR complex and SnRK1 complex) and trehalose pathway (TPS, TPP and TRE) genes in leaves treated with LL ($50 \mu\text{mol.m}^{-2}.\text{s}^{-1}$) and HL ($1000 \mu\text{mol.m}^{-2}.\text{s}^{-1}$) relative to ML ($500 \mu\text{mol.m}^{-2}.\text{s}^{-1}$, control) before (Day 0) and during treatment (Day 1, 2 and 4) using RNAseq. A total of 22 out of 52 sugar sensing transcripts were differentially regulated between all the treatments. For each treatment, analyses were carried on 3 independent biological replicates. We used cut-off values of at least 1CPM in at least 2 samples and a FDR of 0.05 for the differential expression analysis with DESeq2. Blue and yellow lines respectively represent a significant decrease or increase in transcript levels in the treatment compared to the control. Genes were classified based on their respective differential expression as follows (Fold Change compared to control): (Class -3, Highly repressed) $< -5 \text{ FC} <$ (Class -2, Mildly repressed) $< -2 \text{ FC} <$ (Class -1, Slightly repressed) $< 0 \text{ FC} =$ (Class 0, Unaffected) $<$ (Class 1, Slightly induced) $< 2 \text{ FC} <$ (Class 2, Mildly induced) $< 5 \text{ FC} <$ (Class 3, Highly induced).

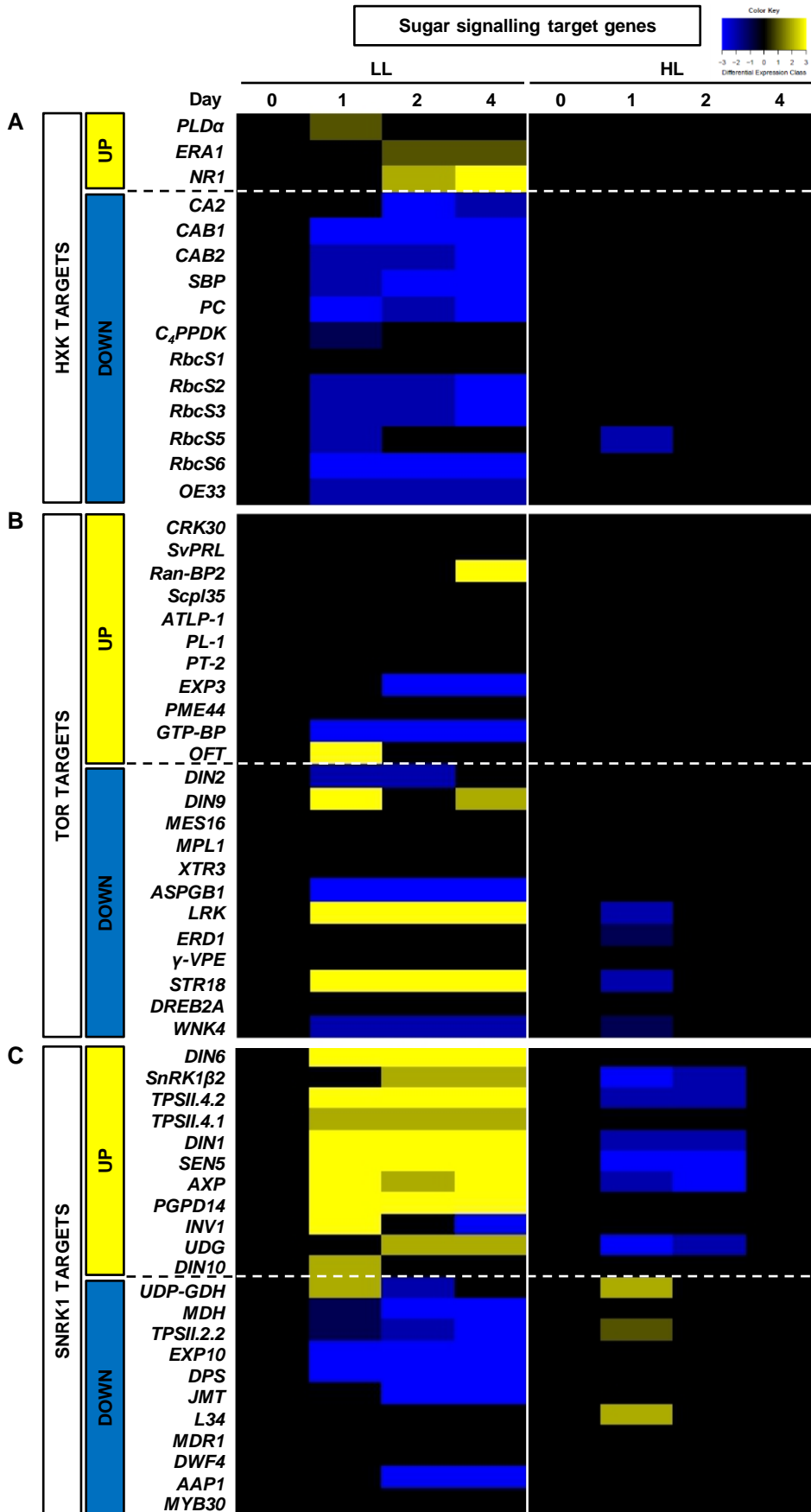


Figure 6: Light treatment had a clear impact on the expression of key HXK and SnRK downstream targets, but no effect on key TOR downstream targets in mature *C₄ S. viridis* leaves. Heatmaps representing the dynamic changes in transcript levels of key downstream targets of HXK (A), TOR (B) and SnRK1 (C) in mature *S. viridis* leaves treated with LL (50 $\mu\text{mol m}^{-2} \text{s}^{-1}$) and HL (1000 $\mu\text{mol m}^{-2} \text{s}^{-1}$) relative to ML (500 $\mu\text{mol m}^{-2} \text{s}^{-1}$, control) before (Day 0) and during treatment (Day 1, 2 and 4). For each treatment, analyses were carried on 3 independent biological replicates. We used cut-off values of at least 1CPM in at least 2 samples and a FDR of 0.05 for the differential expression analysis with DESeq2. Blue and yellow lines respectively represent a significant decrease or increase in transcript levels in the treatment compared to the control. Genes were classified based on their respective differential expression as follows (Fold Change compared to control): (Class -3, Highly repressed) < -5 FC < (Class -2, Mildly repressed) < -2 FC < (Class -1, Slightly repressed) < 0 FC = (Class 0, Unaffected) < (Class 1, Slightly induced) < 2 FC < (Class 2, Mildly induced) < 5 FC < (Class 3, Highly induced).